

# Chapter One

## 1.1 Introduction:

Thermoluminescent dosimeter (TLD) is a passive radiation detection device that is used for personal dose monitoring or to measure patient dose. ATLD measures ionizing radiation exposure by measuring the intensity of visible light emitted from a crystal in the detector when the crystal is heated. The intensity of light emitted is dependent upon the radiation exposure (Yamashita, et al, 1971).

Thermo-luminescence dosimeters (TLD) as radiation detectors imply more than two thousand (2000) types; among them only eight (8) are most common in the field of radiation dosimetry. These eight types which could be divided into tissue equivalent materials which imply Beryllium Oxide (BeO) (Tochilin, et al, 1969), Lithium Borate ( $\text{Li}_2\text{B}_4\text{O}_7$ ), Lithium Fluoride (LiF) (Fowler, et al, 1966) and Magnesium Borate ( $\text{MgB}_4\text{O}_7$ ) with low atomic number (Z) hence have been utilized for medical, personal and industrial applications and the non-tissue equivalent materials that include Calcium Sulphate ( $\text{CaSO}_4$ ) (Yamashita, et al 1971). Calcium Fluoride ( $\text{CaF}_2$ ), Aluminum Oxide ( $\text{Al}_2\text{O}_3$ ) and magnesium orthosilicate ( $\text{Mg}_2\text{SiO}_4$ ) are high atomic number (Z) with high sensitivity used for environmental monitoring.

The TLDs may be used in an extended range of occupational exposures from low level as in conventional radiography to those of high risk such as angiography, nuclear medicine and radiotherapy in addition; any decisions made by regulatory bodies for the workers are based on the results of personal dosimeters in comparison with different dose limits. However, TLD would have a calibration process and as a result, reading or signal stability could be influenced by different factors; these factors imply (temperature, pressure, long term radiation exposure, moisture) and their relevant effects could be expressed in the followings: 1) The effect of heating time in TLD reading (Al-Haj, et al (2004), in a form of glow curve changes which they ascribed to phenomenon of fading which should be less than 5% (Stadtman, et al (2002), and the distortion of the glow curve due to anomalies in routine practice. 2) The temperature: as the TLD read out is sometimes restricted to the applied temperature and dosimeter design such as the thickness (Stadtman, et al (2006). 3) The filter: as it has been used to correct the energydependence of TL material, achieving equivalent doses (used to obtain deep dose rates inside a human body), and filtering out unwanted particles, and 4) to correct for backscatter.

Hence reading of TLD with or without filter will induce significant change in the final measured dose and achieving energy independence in TL phosphors (Pradhan, et al (1979). The applied TLD in radiation dosimeter composed of four different TL phosphors and filters. The first one is a thin Mylar window which gives protection from sunlight exposure and insignificant attenuation to incident radiation and used to measure skin dose. The second filter is a tissue equivalent polymer with a density thickness equal to 1 cm of tissue and utilized to determine the deep dose to an individual as well for whole body external dose. The third filtered TL contains hydrogenous material, such as acrylonitrile butadiene styrene (ABS), to be applicable with neutrons beam. The fourth filter consists of low atomic number material foil such as copper to attenuate any beta particles and to measure only the dose contribution coming from photons (Leon, et al 2009). More factors influencing the TLD reading or signal are the pressure and repeated radiation exposure that could influence even the crystallization of TLD chips. In relation to these influencing factors, (Lee, et al 2015) have developed a technique to reduce the fading effects of repeated radiation exposure in TLD crystal that leads to signal loss of about 15% to only 5%.

The annealing process before usage of TLD in measurement, and as well the nitrogen for cooling have also some influence in TLD reading in addition to spurious effects due to heat exposure, friction and atmosphere (Zimmerman,et al (1966 ).Since the desirable criteria of the phosphors materials used in radiation detectors are: sensitivity, stability of traps and activators and host lattice, long term storage of information, simple glow curve, and spectrum with short wavelength (Fowleras,et al 1966).

TLD materials are not ideal for measuring dose. Many factors have to be taken into account in order to find the most suitable material. The availability is very important as well as the stability of its produced signal. A low fading rate is important (lower than 5% per month) as well as simple glow curves with a plain anneal heating cycle. Although the sensitivity of a tissue equivalent material is not very high, it can be increased by adding impurities called activators. As there are more impurities in the material, more traps are included and thus more light is emitted during thermoluminescence process. Therefore the efficiency of the material is increased.

Except for high sensitivity and efficiency, a low variation in the signal of the background is needed with the aim of measuring low dose thresholds with high accuracy (doses lower than 100  $\mu\text{Gy}$ ). Moreover, a flat energy response over a large range of energies is required.

An ideal dosimeter should have a linear response over a large range of doses and its response should not be affected from the dose rate. Their response variation due to the different angles of the incident radiation to the dosimeter should be well known. Finally, the dosimeter must have small dimensions in order to be able to measure point doses with high spatial resolution (IAEA, 2005).

### **1.2 Problem of study:**

All scintillation materials are subject to radiation damage effects when exposed over prolonged periods to high fluxes of radiation. The damage is most likely evidenced as a reduction in the transparency of the scintillator caused by the creation of color centers that absorb the scintillation light. In addition there may also interference with the processes that give rise to the emission of the scintillation light. Radiation exposures can also induce long lived light emission in the form of phosphorescence that can be troublesome in some measurements.

The damage effects are often observed to be rate dependent and will vary greatly with the type of radiation involved in the exposure. The effects are often at least partially reversible, with annealing taking place even at room temperature over hours or days following the exposure.

### **1.3 Objectives of the study:**

#### **1.3.1 General objective:**

The general objective of this study was to study the factors affecting the reading of thermoluminescencedosimeter (TLD) reading.

#### **1.3.2 Specific objectives:**

- To obtain the glow curve of TLD reading based on different radiation dose.
- To correlate before applied dose and the relative TLD reading with different filters.
- To find the effects of cooling in the acquisition of TLD reading.
- To determine the effects of annealing in TLD measurement.
- To obtain the effects of dose in TLD morphology.

#### **1.4 Thesis outline:**

This study was fall into five chapters, chapter one deals with an introduction, research problem and main objectives of the study. Chapter two highlights the theoretical background of the study in (section one), while discussing literature review at section two. Chapter three elaborates the followed methodology and selective used tools to obtain the results. Chapter four is highlighting the estimated results and outcomes of the study, and finally chapter five contains a detailed discussion of the estimated result, conclusion and researchers recommendations.

## Chapter Two

### Literature Review

#### 2.1 Theoretical Background:

Radiation dosimetry is defined as the measurement, usually, of the absorbed dose, or other relevant quantities like KERMA, exposure or equivalent dose, which is produced due to the interaction of the ionizing radiation with a material. That measurement can be achieved using a dosimeter (Attix, 1986).

A dosimeter with its reader is called a dosimetry system (IAEA, 2005). External dosimetry is a measure of absorbed doses, produced from radiation sources, which are outside of the body of the exposed worker. For this kind of doses a personal dosimeter is used, which is usually called “badge”, and has to be worn by the worker every time that he/she is exposed to the radiation, in order to make sure that a reference limit is not exceeded. If a worker works with sources which are not sealed, then the radioactive material gets into his/her body and absorbed by tissues or organs in the body. Therefore, internal doses should also be measured, using specific monitors, with the aim of calculating the total effective dose to the worker from internal and external exposures (IAEA, 2004).



Absolute dosimeters are used in order to measure directly the dose without the need of a calibration in a known radiation field (e.g. calorimeters) (Attix, 1986). On the other hand, secondary or relative dosimeters provide indirect measurement of dose but have to be calibrated using a primary (absolute) dosimeter at reference conditions. An example of secondary dosimeters is the TLDs (thermoluminescence dosimeters) which are normally calibrated using an ion chamber dosimeter (McKinley, 1981).

TLDs have been developed significantly over the years and a lot of materials were studied to see if they are suitable for applications for different areas in dosimetry (McKinley, 1981). TL materials store energy inside their structure when they are irradiated, as electrons and holes are trapped in trapping centers due to defects. When that material is heated, electrons and holes recombine, at luminescence centers, and thus light is emitted. The light is measured using a PMT (photomultiplier tube) inside the reader device (Dam, et al (2006).

The photons which are emitted are in the visible region and they comprise the TL signal. Preferably, one photon is emitted from each trap center.

Therefore, the measured signal is an index of the number of electron/hole pairs and it is proportional to the absorbed dose (Knoll, 2000).

TLDs are mainly used for personal monitoring of workers who are exposed to radiation that is higher than 3/10 of the dose equivalent limits.

The individual monitoring of those workers is essential in order to make sure that the limit of the equivalent dose does not exceed the maximum permissible dose (McKinley, 1981). They are used to determine the dose of an individual at a specific depth of his/her body, most of the times at 0.07 and 10 mm. At 0.07 mm the effective dose of the worker's skin ( $H_p(0.07)$ ) and at 10 mm the dose of the organs inside the body ( $H_p(10)$ ) is measured. Additionally, at depth 3 mm the dose in the eyes of a worker is calculated (IAEA, 2004).

TLDs can also be used for environmental, neutron and clinical monitoring. Moreover in vivo techniques, in radiotherapy as well as in diagnostic radiation measurements. Furthermore, for dating of materials and for analysis of the meteorites (McKinley, 1981).

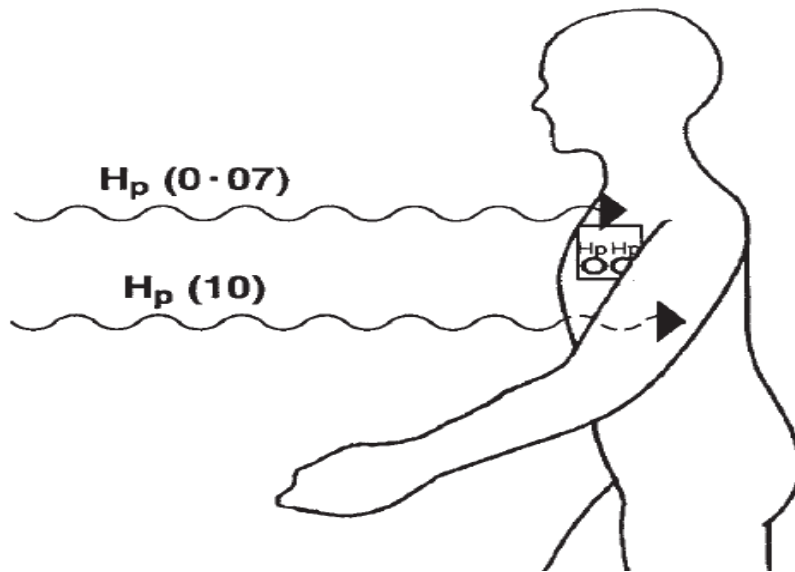


**Figure 2.1: External exposure – Estimation of dose at depths equal to 0.07 and 10 mm.**

### **2.1.1 Types of thermoluminescent dosimeter:**

Thermo-luminescence dosimeters (TLD) as radiation detectors imply more than two thousand (2000) types; among them only eight (8) are most common in the field of radiation dosimetry. These eight types which could be divided into tissue equivalent materials which imply Beryllium Oxide ( $\text{BeO}$ ) (Tochilin et al, 1969), Lithium Fluoride ( $\text{LiF}$ ) Fowler and Attix, (1966), and Magnesium Borate ( $\text{MgB}_4\text{O}_7$ ) with low atomic number ( $Z$ ) which consider as tissue equivalent materials and the non-tissue equivalent materials imply Calcium Sulphate ( $\text{CaSO}_4$ ) (Yamashita et al, 1972).

Calcium Fluoride ( $\text{CaF}_2$ ), Aluminum Oxide ( $\text{Al}_2\text{O}_3$ ) and magnesium orthosilicate ( $\text{Mg}_2\text{SiO}_4$ ) which are high atomic number (Z) with high sensitivity and used for environmental monitoring.

The most widely used material is the LiF with added magnesium and titanium,  $\text{MgB}_4\text{O}_7$  has similar behavior as LiF with higher sensitivity (5-10 times higher than LiF). Its disadvantage is that an additional anneal irradiation is needed to reduce the fading as it is very sensitive to light.  $\text{Li}_2\text{B}_4\text{O}_7$  has less sensitivity compared with LiF (1/10th of LiF) and is hygroscopic. BeO is a more tissue equivalent material than LiF with almost the same sensitivity, but toxic and very sensitive to light. (Dam, et al, 2006).

The TLDs may be used in an extended range of occupational exposures from low level as in conventional radiography to those of high risk such as angiography, nuclear medicine and radiotherapy in addition; any decisions made by regulatory bodies for the workers are based on the results of personal dosimeters in comparison with different dose limits.

However, TLD would have a calibration process and as a result, reading or signal stability could be influenced by different factors; these factors imply (temperature, pressure, long term radiation exposure, moisture).

### **2.1.2 Lithium Fluoride:**

Thermoluminescent materials such as lithium fluoride (LiF) provide a simple inexpensive method of measuring radiation dose over an extended period of time. Normally when energy is applied to an electron, it will move up to a higher energy state (orbital), then drop back to its ground state releasing the excess energy.

Crystals of LiF have meta stable energy state in which excited electrons may be trapped for periods up to 80 years. Heat applied to the crystal will raise the electron out of the meta-stable trap, allowing it to revert

Lithium fluoride has now been used for more than 30 years as detectors for thermoluminescence dosimetry back to its ground state by emitting the excess energy as photons. About 30 methods and compositions are known for the fabrication of LiF-based phosphors. In most cases lithium fluoride is used in the form of pressed and polycrystalline tablets as well as in the form of items made of Teflon with LiF powder dispersed in it. All of these detectors have one inherent drawback: a considerable background signal which is determined by the large surface in contact with the surrounding atmosphere.

In single-crystal detectors this disadvantage is eliminated because of the small surface of interaction with the atmosphere, transparency over a wide region of the spectrum, and as a consequence of these properties a small value of the background signal, as well as an increase in the sensitivity of the detector. The application of such detectors, however, has been limited by the difficulty of obtaining large lithium fluoride single crystals that would have a uniform sensitivity. LiF is an alkali halide with atomic number equal to 8.2 (close to 7.4 of the human tissue) and is widely used for personnel monitoring. It can be found in many forms namely chips or pellets, single crystals, rods, powders, ribbons and gel. A LiF crystal doped with magnesium and titanium. Magnesium is used to increase the number of traps in the lattice and titanium is used in order to increase the number of luminescence centers.

## **2.2 Components of TLD:**

The body TLD comprises a TLD card, wrapper and holder. The TLD card is of Harshaw<sup>TM</sup> design and contains two pellets of specially doped lithium fluoride (LiF:Mg,Cu,P). The thicker element is used for the assessment of the dose from strongly penetrating radiation and the thinner one for the assessment of the dose from both weakly- and strongly penetrating radiation.

These are covered front and back with a thin retaining layer of PTFE (polytetrafluoroethylene). The cards are individually bar coded.

The wrapper protects the dosimeter from contamination by chemicals, dirt or radioactive materials, and is of aluminized polyester. It carries printed wearer and identifier information, in text and bar-code formats.



Figure 2.2: Components of TLD

### 2.3 TLD Reader:

A TLD is a phosphor, such as lithium fluoride (LiF) or calcium fluoride (CaF), in a solid crystal structure. When a TLD is exposed to ionizing radiation at ambient temperatures, the radiation interacts with the phosphor crystal and deposits all or part of the incident energy in that material.

Some of the atoms in the material that absorb that energy become ionized, producing free electrons and areas lacking one or more electrons, called holes. Imperfections in the crystal lattice structure act as sites where free electrons can become trapped and locked into place.

Heating the crystal causes the crystal lattice to vibrate, releasing the trapped electrons in the process. Released electrons return to the original ground state, releasing the captured energy from ionization as light, hence the name thermoluminescent. Released light is counted using photomultiplier tubes and the number of photons counted is proportional to the quantity of radiation striking the phosphor.

Instead of reading the optical density (blackness) of a film, as is done with film badges, the amount of light released versus the heating of the individual pieces of thermoluminescent material is measured. The "glow curve" produced by this process is then related to the radiation exposure. The process can be repeated many times.

### **2.3.1: TLDS to measure body doses:**

Many dosimetry services, both large and small, use TLDs as a convenient means of monitoring whole body exposure to beta, X and gamma radiations.



Dosimeters vary in design but typically comprise two or more LiF detectors. These can be chips, discs in a polytetrafluoroethylene (PTFE) matrix, or powders. They are used in cards designed for automated readout. A reader decodes holes in the card which provide information about the wearer; it heats the TLD and measures the light emission. The TLDs are then annealed and reused. It is important to keep the discs clean and dry. Personal details about the wearer can be printed on the outside of the dosimeter. The shape of the card ensures that it is correctly located inside a holder by the user. Some of the discs must be used behind filters to simulate measurements of Hp (0.07) and Hp (10).

In general, TLDs are not designed to provide discrimination between the types and energies of radiations and the lack of qualitative data places greater responsibility on the user to ensure that it is correctly used and not contaminated. TLDs are less affected than film badges by fading and ambient conditions. Consequently, they are more appropriate for wearing periods of up to three months. They are also more suitable, but not ideal, dosimeters for mixtures of weakly penetrating (less than 500 keV) beta and (less than 20 keV) photon radiations, (Faiz M. Khan (2003)).



Figure 2.3: Body thermoluminescencedosimetry (TLD)

### **2.3.2 Assessment of external exposures:**

Personal dosimeters are designed to measure the dose in soft tissue at a defined depth below a specified point on the body. The quantity personal dose equivalent  $H_p(d)$  is normally determined at two depths,  $d = 0.07$  and 10 mm, as measures of exposure to weakly and strongly penetrating radiations respectively. The former is representative of dose to skin and the latter represents dose to the blood forming organs. If exposure to the eye is of particular concern, a depth of 3 mm represents the eye lens the personal dose equivalent at 10 mm depth,  $H_p(10)$ , is used to provide an estimate of effective dose for comparison with the appropriate dose limits.

As  $H_p(0.07)$  is used to estimate the equivalent dose to skin, it should be used for extremity monitoring, where the skin dose is the limiting quantity.

### **2.3.3 TLDs to measure extremity doses:**

Some work may expose the extremities or other parts of the body to significantly more radiation than the whole body receives. Examples include the manipulation of short range, energetic sources; situations in which extremity shielding is impractical; and work that involves parts of the body being closer to collimated radiation beams. In such circumstances, TL materials are used to measure the doses to specific parts of the body. The discs mentioned are less than 15 mm in diameter by 0.5 mm in thickness and chips are 3 mm square by 1 mm in thickness. Rods of a size of 1 mm by 6 mm and extruded lithium fluoride ribbons are also available. They may be contained in unobtrusive rings and fingerstalls (F) to measure finger doses. Powders require careful handling to avoid inducing thermoluminescence by grinding or shaking, but sachets containing just a few milligrams may be fitted to straps and worn on the wrist (W) or ankle or as a headband (H) (Stadtman, et al (2006)).

## **2.4 Advantages of TLD:**

- a) They are tissue equivalent
- b) They are available in many forms
- c) They have small size and they can be used for point dose measurements.
- d) They have large range of dose
- e) Their response is not depended on the dose rate.

## **2.5: Uncertainty of TLD:**

An essential aspect of quality assurance in individual monitoring is assessing the quality of the measurement results. In other words to what extent is it reasonable to believe that the reported number is a good estimate of the true dose value. The greater this belief, the confidence or probability that the measured value is within a certain defined range around the true value, or rather that the true value is within a certain range of the observed value, the better the quality of the measurement. A required quality can often be expressed as a combined standard uncertainty or as an expanded uncertainty with a coverage factor of 2, or in a more general probabilistic approach, by a coverage interval, with in general a 95% coverage probability.

In the evaluation of the uncertainty, all knowledge of the dosimeter and evaluating system (TLD-readers, densitometers, track counting systems) both from experience and from type testing should be used possibly in combination with information from the client/customer such as local exposure and storage conditions. Evaluating the uncertainty in measurement is quantifying the quality of measurement.

## **2.2 Previous Studies:**

This chapter deals with the previous studies carried out by some authors about the general effects of ionizing radiation on the plasticized (plastic) materials such as polymers, and crystallized chips.

In such realm Said (2013), conducted study done in the Effects of gamma irradiation on the crystallization, thermal and mechanical properties of Poly(L-Lactic Acid)/Ethylene-co-Vinyl Acetate (PLLA/EVA) blends after receiving 100 kGy. They revealed the induced effects by Differential Scanning Calorimetry (DSC) and Thermogravimetric analysis (TGA) as crystallization behaviors and thermal stability before and after exposed to different doses of gamma irradiation. The effect of degradation in form of weight loss for EVA and PLLA/EVA blend has been shown in clearly in Figure (4 & 5) which revealed that: the hydrolytic degradation rate of PLLA/EVA blend can be widely controlled by exposing the PLLA/EVA to gamma irradiation and also by EVA content.

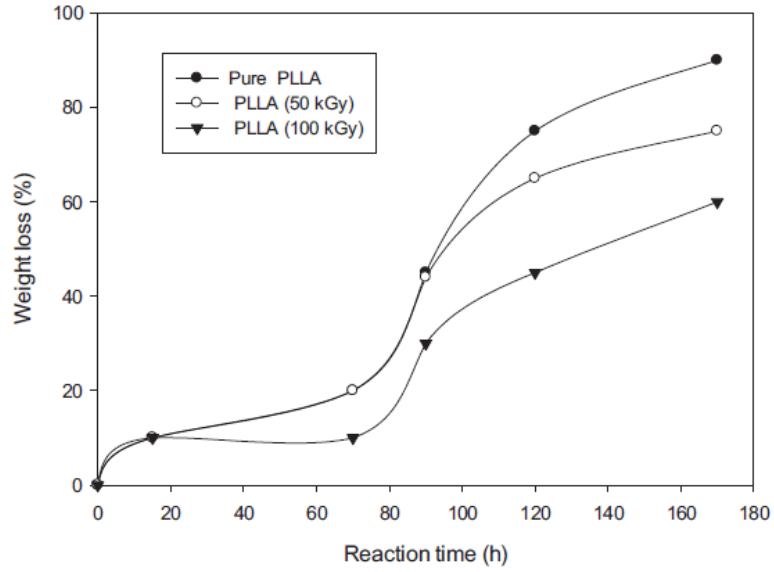


Figure 2.4: Weight loss (%) of PLLA before and after exposed to gamma irradiation (Hossam, 2013)

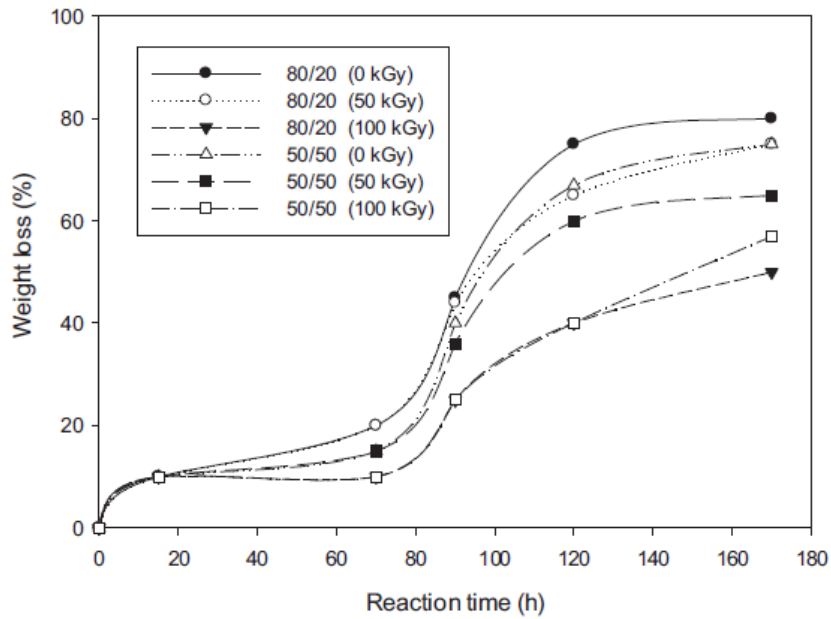


Figure 2.5: Weight loss (%) of polymer blends PLLA/EVA before and after exposed to gamma irradiation (Hossam, 2013).

One more radiation effect was the tensile strength which was greatly dependent on the ratio of EVA content in the blend. 80% PLLA/20% EVA polymer blend exhibits maximum tensile strength and ductility compared with other blends possibly due to the relative interaction between PLLA and EVA at this ratio. The strain-at-break was gradually increased up to 50 wt% of EVA and then suddenly increased at 80 wt% of EVA. After being irradiated by 50 kGy, the tensile strength and modulus are enhanced greatly, whereas the elongation at break is reduced slightly. The microstructural changes occurring in polymeric chain (PLLA and EVA) due to gamma irradiation with the increasing the radiation dose from 0 kGy to 100 kGy, the absorption peak of CH<sub>3</sub> + C-C (913 cm<sup>-1</sup>) of PLLA decays and the shape of absorption peaks of C=O (1751 cm<sup>-1</sup>), symmetric CH<sub>3</sub> (1373 cm<sup>-1</sup>), and asymmetric COC (1180 cm<sup>-1</sup>) changes, indicating the interaction between PLLA and EVA. The degree of crystallinity (X<sub>c</sub>) of the PLLA phase indicated that PLLA and EVA were immiscible over the composition range investigated. However, there is a sharp decrease in the crystallinity with increasing EVA and irradiation dose. The effect of the irradiation dose on the thermal stability was found to depend on the PLLA/EVA ratio.



The weight loss (%) increased as the ratio and the irradiation dose decreased. However, the weight loss (%) decreased as the ratio increased, especially beyond 330 °C. The increase in thermal stability associated with an increasing ratio is due to the increased (cross linking) that occurs upon the removal of acetic acid. These effects have been obviously shown in Figure (6, 7, 8).

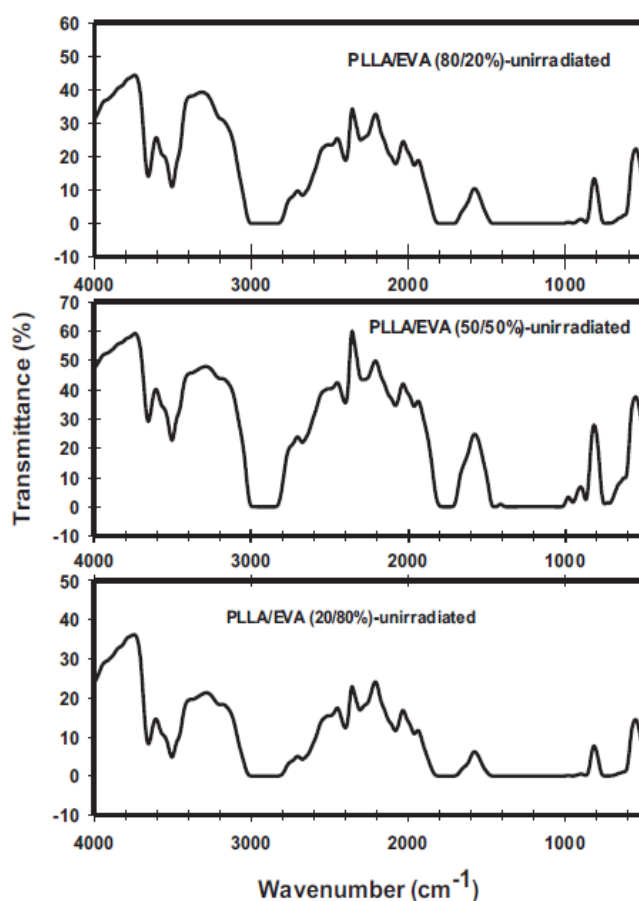


Figure 2.6 IR spectra of thin films of unirradiated PLLA/EVA blends (Hossam, 2013).

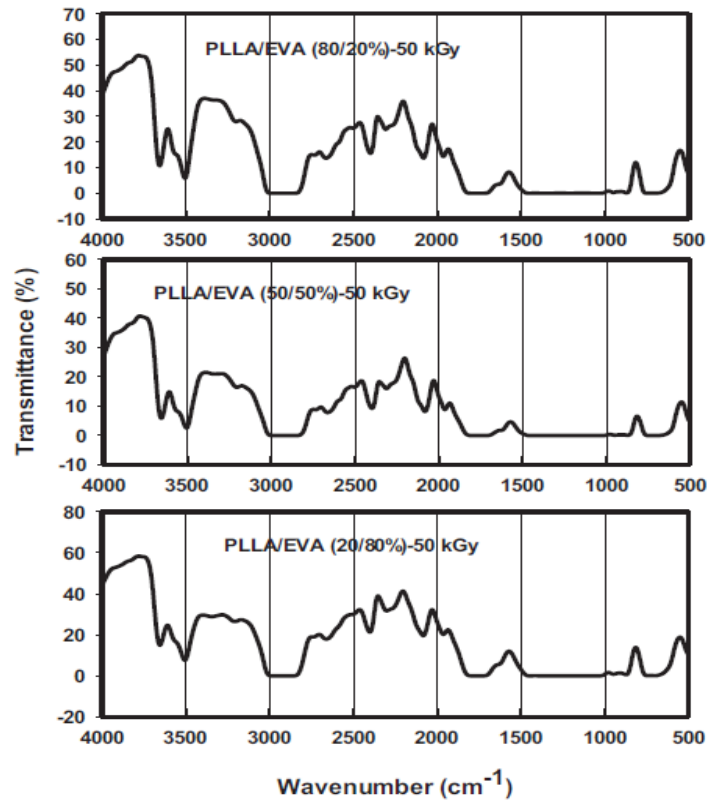


Figure 2.7: IR spectra of PLLA/EVA blends gamma irradiated at a dose of 50 kGy (Hossam, 2013).

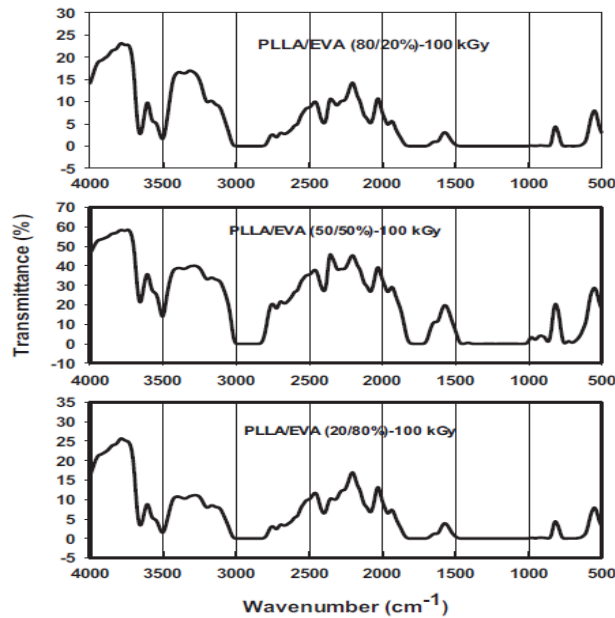


Figure 2.8: IR spectra of PLLA/EVA blends gamma irradiated at a dose of 100 kGy (Hossam, 2013).

On the study done by Kalidasan et al, (2015) where gamma irradiation (5, 10, and 20 kGy) of sodium borate single crystals  $\text{Na}_2[\text{B}_4\text{O}_5(\text{OH})_4] \cdot (\text{H}_2\text{O})_8$  (monoclinic system) showed the induced effects as crystal defect which in turn influence thermo-luminescence glow curves and as well the vibrational modes of the sodium borate single crystals, dielectric permittivity, conductance and dielectric loss versus frequency graphs of these crystals have been analyzed to know the effect of gamma ray irradiation on these parameters:

The x-ray rocking curves confirm the formation of defects after gamma ray irradiation in the sodium borate single crystals, where the crystallinity being reduced following irradiation towards the amorphous state (Figure 6). And the thermo-luminescence glow curves due to gamma ray induced defects have been observed with tortuously and increases following the irradiation dose (Figure 9). While the molecular structure also has been noticed in an increasing mode at 5 kGy, then decreased for 10 kGy and totally vanish at 20 kGy; however the increment of Raman intensity could be ascribed to charge localization and enhancement in the saturation of bonds (Figure 10).

Even the properties such as conductance, dielectric, and di-electric permittivity versus applied frequency graphs showed the sign of reduction and defects at 10 KGy of gamma irradiation (Figure 11).

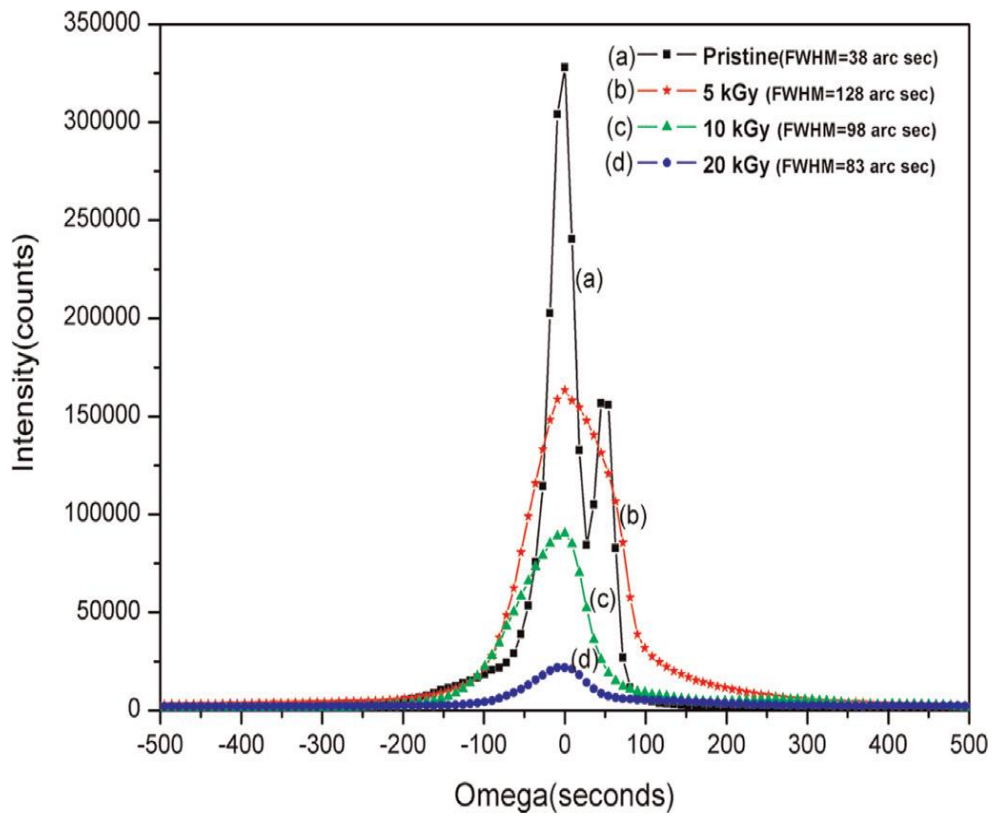


Figure 2.9: X-ray rocking curves of pristine and 5, 10,20kGy doses of gamma ray irradiated sodium borate single crystals.

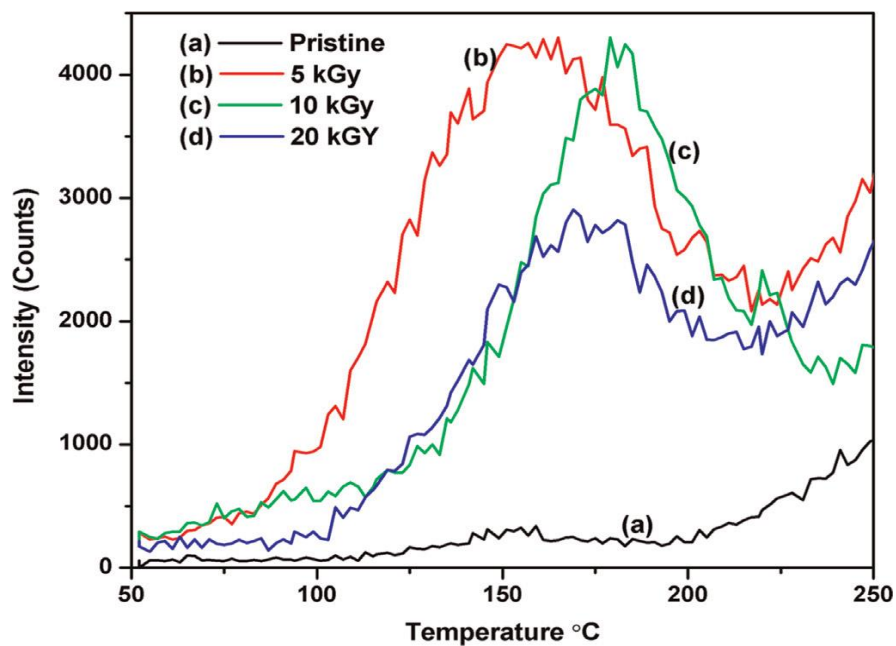


Figure 2.10: Thermo-luminescence spectra of pristine and 5, 10, 20 kGy doses of gamma ray irradiated sodium borate single crystals.

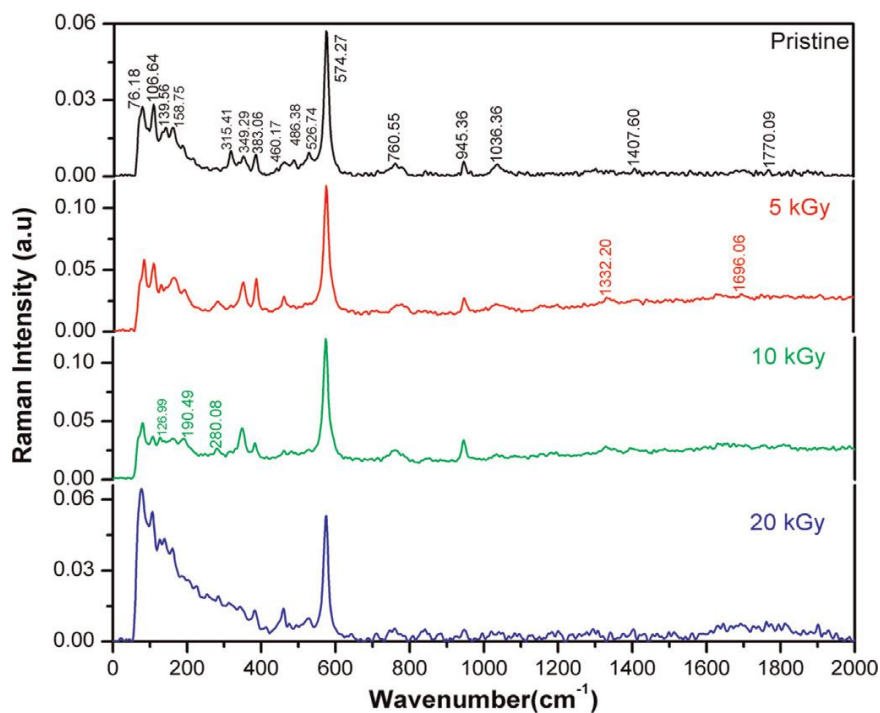


Figure 2.11: FT-Raman spectra of pristine and 5, 10, 20 kGy doses of gamma ray irradiated sodium borate single crystals

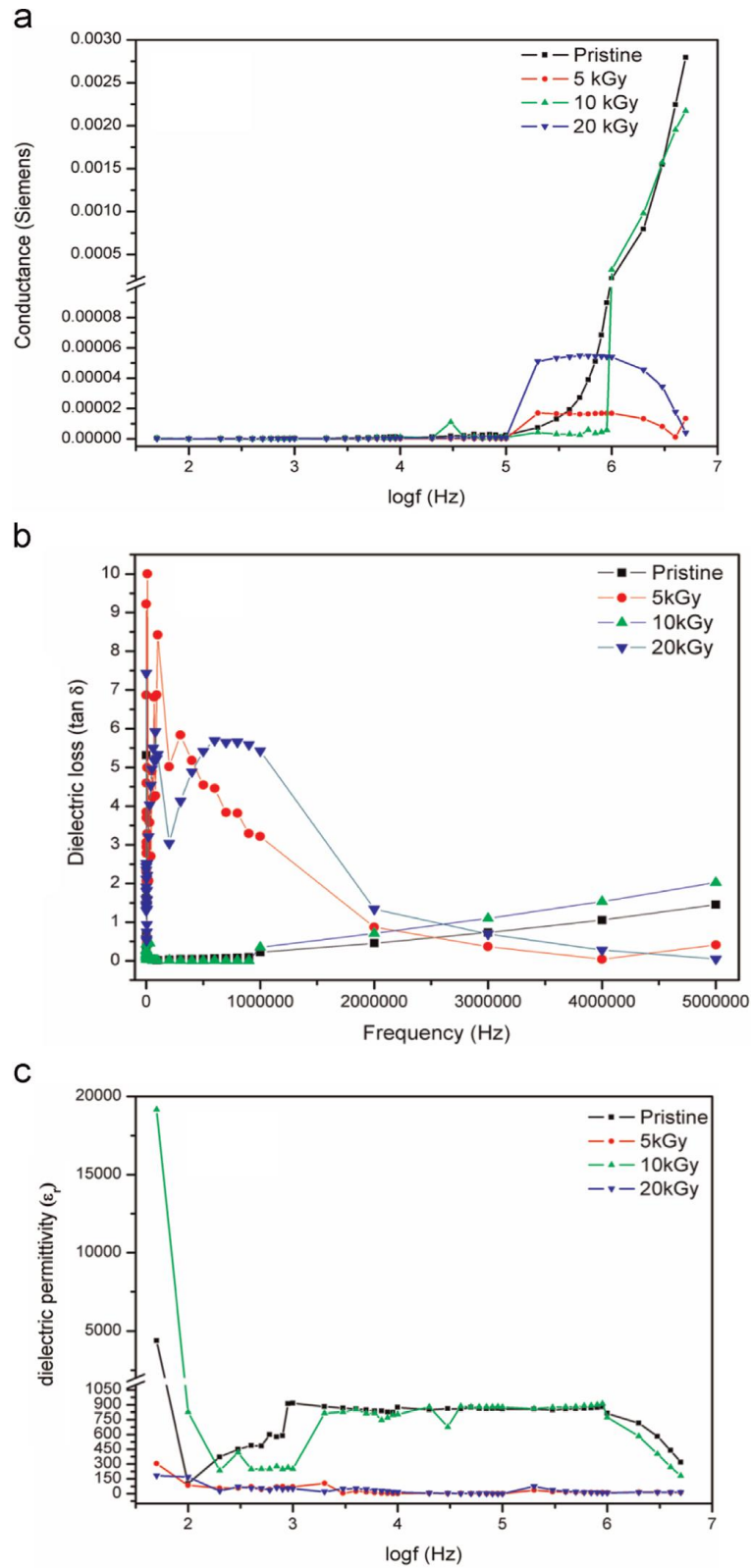


Figure 2.12: Variation of conductance (a), dielectric loss (b), and dielectric versus permittivity (c) versus frequency of pristine and 5, 10, 20 kGy doses of gamma ray irradiated sodium borate single crystals.

Dey et al, (2014) showed the effects of gamma irradiation (50, 100, 150, 250 and 500 krad) in the Blend film of polyvinyl alcohol (PVA), in which they found that: the tensile strength of pure PVA film increases following the increment of radiation dose and the highest tensile strength (32MPa) for blends was observed for 5% gelatin containing PVA film at 50 Krad which was 19% higher than that of non-irradiated blend (Figure 13) and the elongation at break for both pure and blended PVA were increased following the irradiation increment up to the highest elongation break (165%) for 10% gelatin containing PVA film at 100 Krad as shown in Figure (14), then the elongation at break decreased with the increase of radiation doses due to radiation induced degradation.

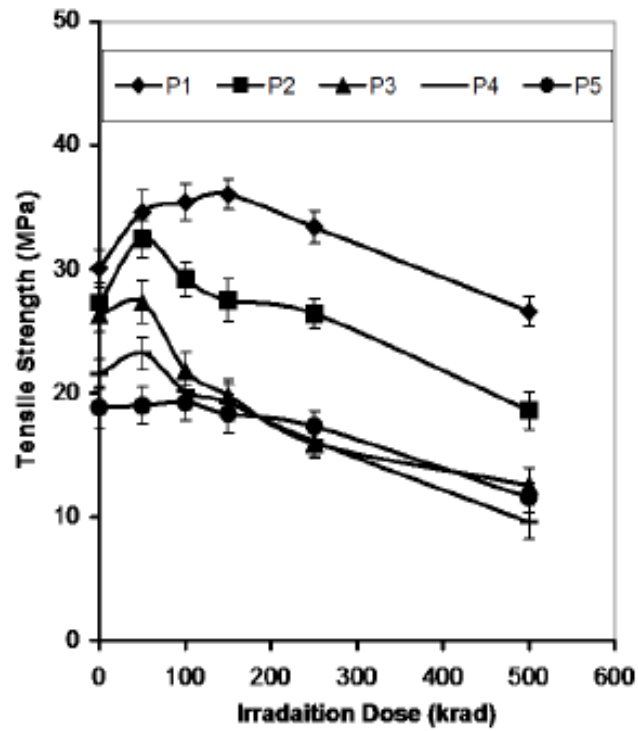


Figure 2.13: Tensile strength (TS) of PVA based gelatin film against different gamma irradiation dose (Krad).

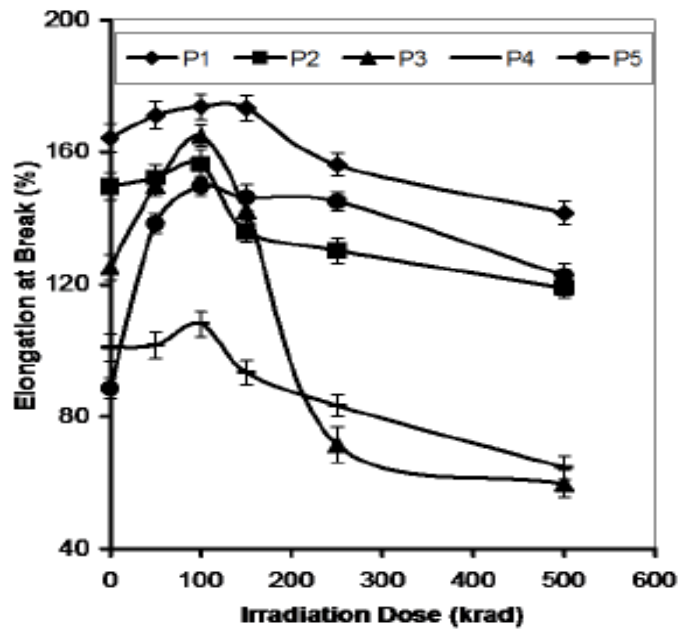


Figure 2.14: Elongation at break (Eb) of PVA based gelatin film against different gamma irradiation dose (Krad).



In the same realm, Sen et al, (2003) showed the degradation of commercial isobutylene-isoprene rubbers after irradiated by gamma radiation (10 kGy) in view of viscosity loss significantly up to 100 kGy of irradiation dose with no further change beyond this dose. However with the presence of air; degradation has been observed even at low dose relative to N<sub>2</sub> presence as shown in Figure (15).

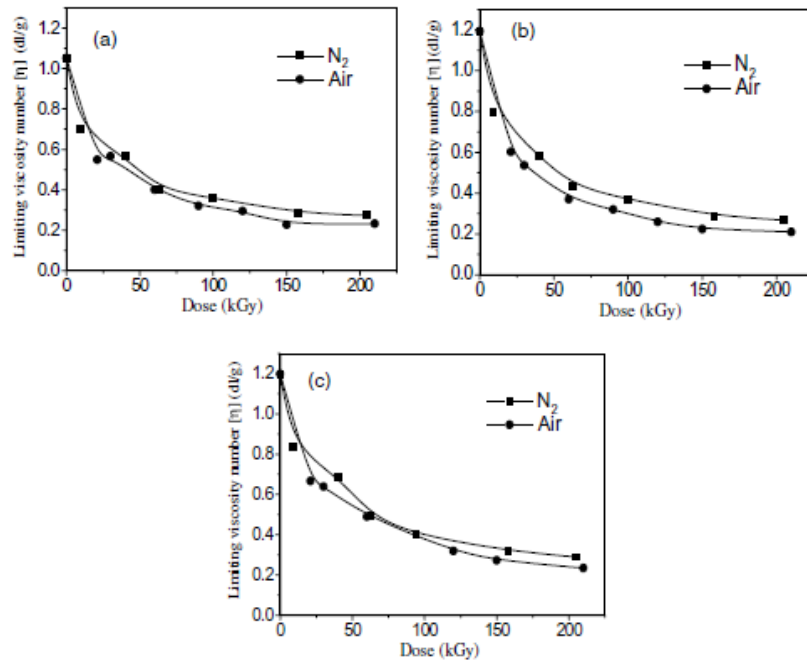


Figure 2.15: shows the variation of limiting viscosity numbers with irradiation dose, for low dose rate irradiation (0.18 kGy/h) in air and N<sub>2</sub>; (a) Ex165, (b) Ex 268, (c) BK1685N (Sen et al, 2003).

Other radiation effects have been studied by Sandra et al, (2013) as controlled degradation of isoprene/isobutene in rubbers for recycling purposes; in which they evaluated gamma-irradiation effects for re-use or recycling purposes in elastomeric bromobutyl compositions irradiated at 5, 15, 25, 50, 100, 150 and 200 kGy. They revealed that: The elongation at break has been reduced obviously following radiation dose from 5-200 KGy due to chain scission as in Figure (16), while the tensile strength showed a gradual reduction even at low doses (5 KGy) which is ascribed to prevalence of bond scission leading to consequent mass molar reduction (Figure 17); however for doses from 5 to 25 kGy; scission and cross linking simultaneous could be observed as co-events and for doses above 50 kGy; the prevalence of chain scission and further polymeric chain degradation were observable.

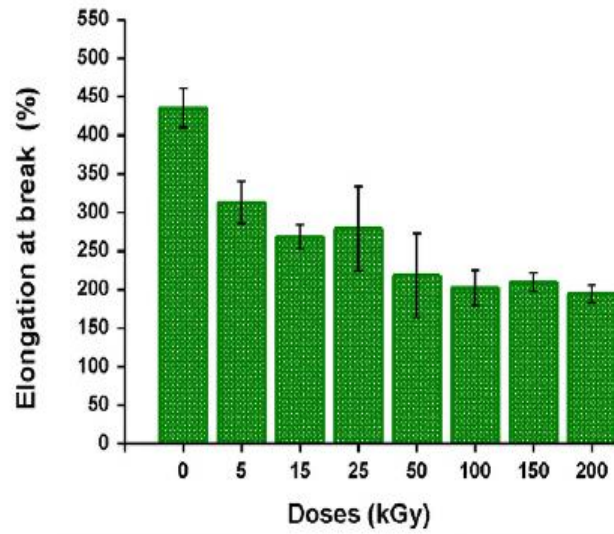


Figure 2.16: Elongation at break for irradiated and non-irradiated Bromobutyl rubber.

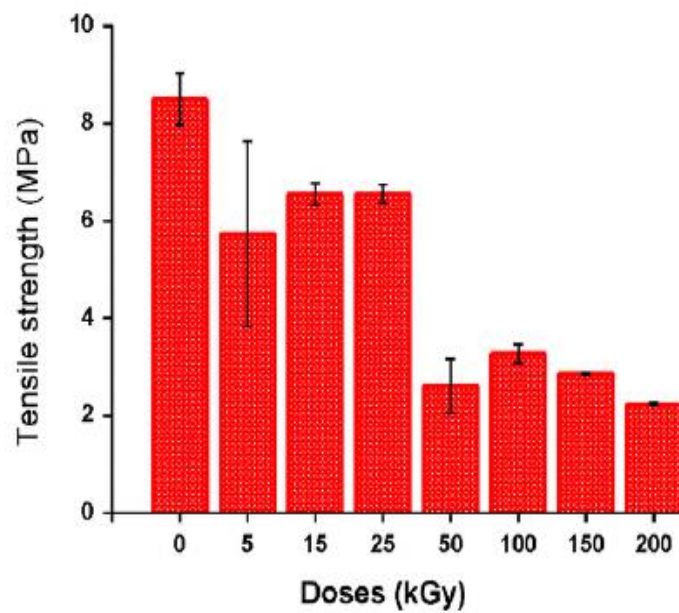


Figure 2.17: Tensile strength for irradiated and non-irradiated Bromobutyl rubber.

The general ionizing radiation effects on bio and/or organic compounds have been summarized in by Fried (2003) with relative examples as shown in Table (2.1)

Table 2.1: shows Effects of Environmental Agents on Polymers (Fried J.R, 2003)

| <b>Agent</b>              | <b>Susceptible polymer</b>   | <b>Example</b>                            |
|---------------------------|--|---|
| Biodegradation            | Short-chain polymers,<br>Nitrogen-containing polymers,<br>polyesters | Polyurethanes, polyether-<br>polyurethane |
| Ionizing radiation        | Aliphatic polymers having<br>quaternary carbon                       | PMMA, polyisobutylene                     |
| Moisture                  | Heterochain polymers   | Polyesters, polyamides<br>polyurethanes   |
| Organic liquid and vapors | Amorphous polymers   | Polystyrene, PMMA                         |
| Ozone                     | Unsaturated elastomers   | Polyisoprene, polybutadiene               |
| Sunlight                  | Photosensitive polymers  | Polyacetals, polycarbonate                |

In the field of radiation measurement (dosimetry), the TLD has been mostly applicable with only eight common types as (Beryllium Oxide (BeO) (Tochilin et al, 1969), Lithium Borate ( $\text{Li}_2\text{B}_4\text{O}_7$ ), Lithium Fluoride (LiF) Fowler and Attix, (1966), and Magnesium Borate ( $\text{MgB}_4\text{O}_7$ ) with low atomic number (Z)) which consider as tissue equivalent materials and the non-tissue equivalent materials imply Calcium Sulphate ( $\text{CaSO}_4$ ) (Yamashita et al, 1972), Calcium Fluoride ( $\text{CaF}_2$ ), Aluminum Oxide ( $\text{Al}_2\text{O}_3$ ) and magnesium orthosilicate ( $\text{Mg}_2\text{SiO}_4$ ) which are high atomic number (Z) with high sensitivity and used for environmental monitoring.

The ionizing irradiation also has an impact on the crystallinity, in such realm, the PVA crystallinity has been reduced due to  $\gamma$ -irradiation (100 kGy) towards amorphous phase as shown in x-ray diffraction spectrum (Figure 18), in which the pattern of XRD intensity peaking at  $2\theta = 19.66^\circ$  decreases gradually from control to irradiated samples and shifts to the lower angle side with another intensity peaking at  $2\theta = 22.76^\circ$  which in turn increases gradually with the increase of dose. This result may reflect the fact that the polymer matrix suffer from some kind of structural rearrangement due to irradiation treatments.

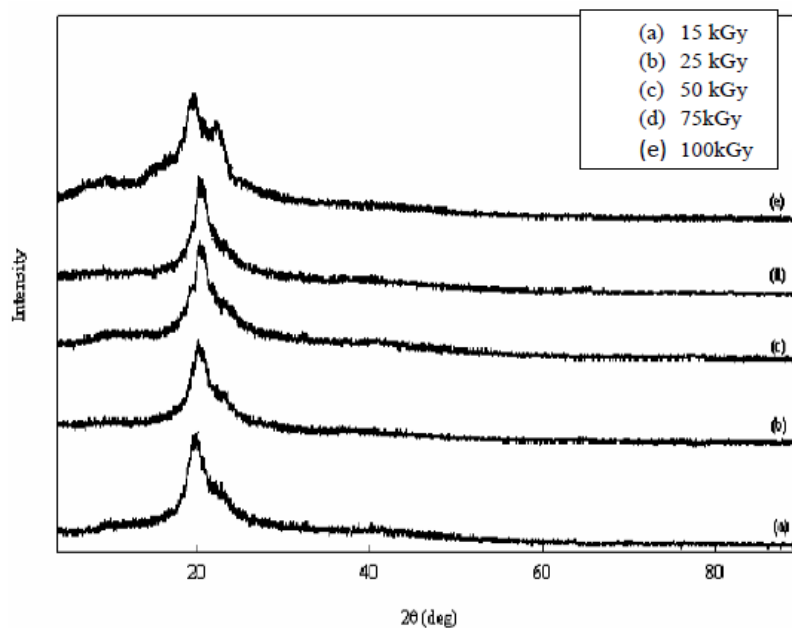


Figure 2.18: Shows amorphous phase in XRD spectrum of PVA irradiated at different doses

The effects of  $\gamma$ -radiation on PVA crystallinity (Figure 19) have been also studied by Mohammed et al, (2011); in which the dominant peak of XRD pattern of pure PVA film irradiated at different doses up to 50 kGy shows a prominent peak at  $2\theta = 19.5^\circ$ , corresponding to the typical crystallinity of PVA as discussed in the literatures (Bhat et al., 2005; Asri, 2005). The smooth XRD pattern indicates that the pure PVA samples have no scattering influenced to the spectra due to its pureness. When it was irradiated with  $\gamma$ -rays, there is continuous reduction of the crystalline structure towards amorphous phase at higher dose of 50 kGy.

The crystallinity of PVA was destroyed with increasing dose suggesting that the PVA backbone alignment could be hindered by bond scission of the C-H and C-OH side chains.

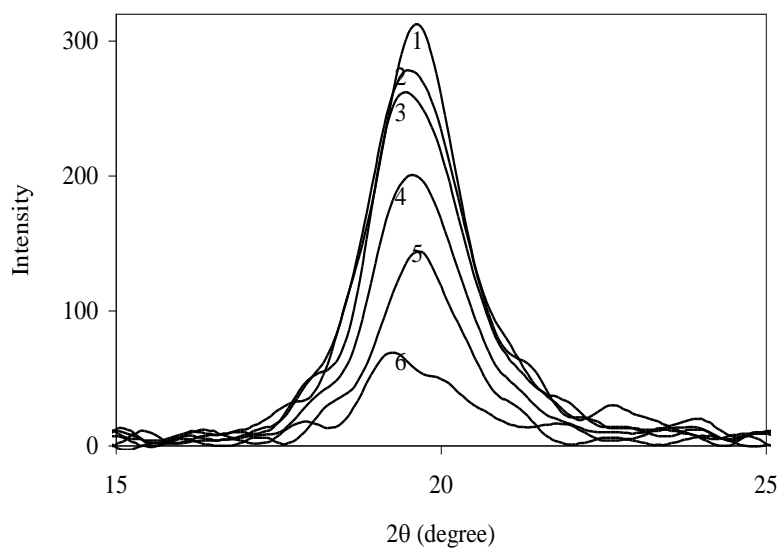


Figure2.19: shows the XRD spectrum of pure polyvinyl alcohol PVA irradiated at different doses.

Therefore from the general highlighted literature; the irradiation effect could be generalized to imply all organic compounds as well as those utilized in radiation dosimetry such air, TLD crystal or etc ... which in turn will influence the persistence, consistence, accuracy and sensitivity of measurement.

## **Chapter Three**

### **Materials and Methods**

#### **3.1 Place and time of the study:**

This study was done in Radiation Isotopes Center of Khartoum (RICK), in the period between (2014-2017).

#### **3.2 Materials:**

- TLD pellets and their holder (LiF: Mg: Ti).
- Manual TLD-Reader RA'04 is Reader-Analyzer new system which used in this study.
- Annealing oven for thermo luminescent dosimeter.
- Gamma radiation source which was Cs-137 source.
- Reference Ionization Chamber.
- Scanning electron microscope SEM.

##### **3.2.1 Scanning electron microscope SEM:**

A scanning electron microscope (SEM) is a type of electron microscope that produces images of a sample by scanning the surface with a focused beam of electrons. The electrons interact with atoms in the sample, producing various signals that contain information about the sample's surface topography and composition.



The electron beam is scanned in a raster scan pattern, and the beam's position is combined with the detected signal to produce an image. SEM can achieve resolution better than 1 nanometer. Specimens can be observed in high vacuum in conventional SEM, or in low vacuum or wet conditions in variable pressure or environmental SEM and at a wide range of cryogenic or elevated temperatures with specialized instruments.

The most common SEM mode is detection of secondary electrons emitted by atoms excited by the electron beam. The number of secondary electrons that can be detected depends, among other things, on specimen topography. By scanning the sample and collecting the secondary electrons that are emitted using a special detector, an image displaying the topography of the surface is created. The signals used by a scanning electron microscope to produce an image result from interactions of the electron beam with atoms at various depths within the sample. Various types of signals are produced including secondary electrons (SE), reflected or back-scattered electrons (BSE), characteristic X-rays and light (cathodoluminescence) (CL), absorbed current (specimen current) and transmitted electrons.

Secondary electron detectors are standard equipment in all SEMs, but it is rare that a single machine would have detectors for all other possible signals.

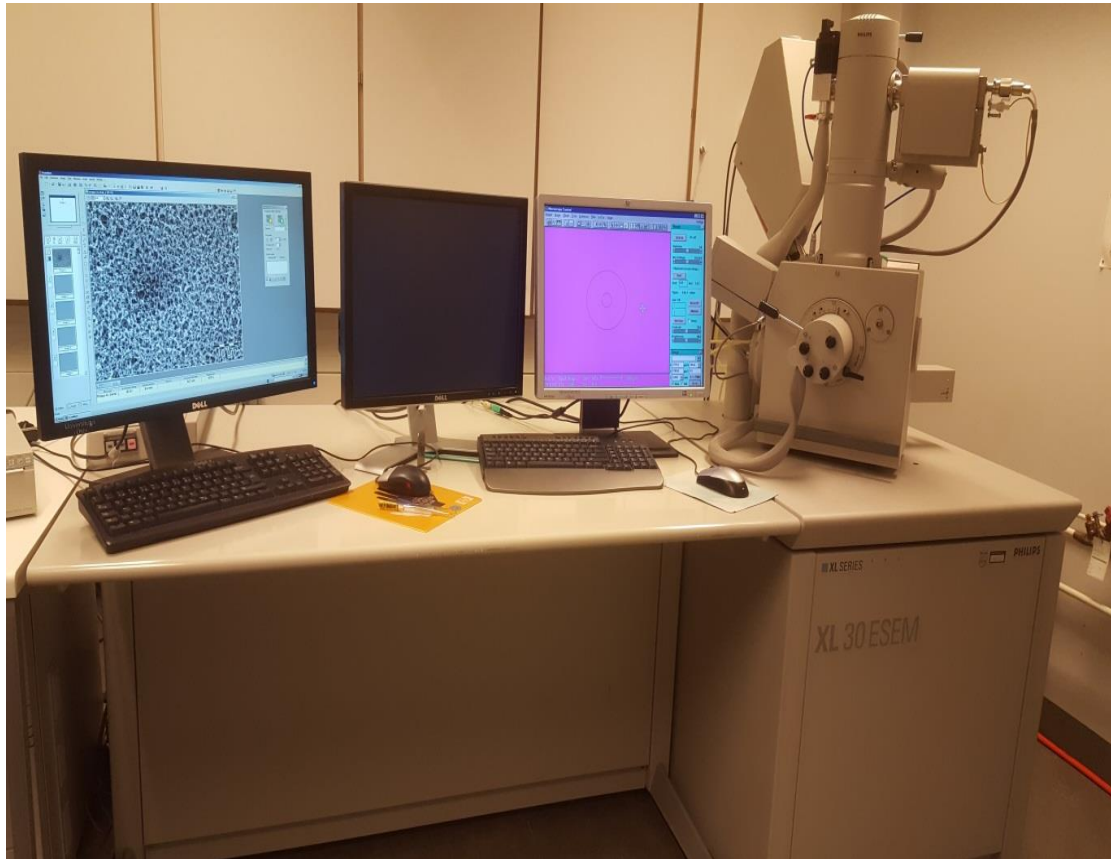


Figure 3.1 Shows the Scanning electron microscope

### **3.2 Method:**

In this study a total of fifty TLDs chip have been used, situated in 25 holders each fit for two pellets defined as shallow dose Hp (0.07) and deep dose Hp (10).

All pellets have been used with and without annealing at oven up to 400°C, with/without build up(Hp 0.07 &Hp 10), with/without cooling by nitrogen flux.

For measuring the zero doses (ZD), the TLDs placed on the tray of stainless steel which inserted to the oven (400°C), then followed by fast cooling using nitrogen flux in some case and without cooling in other. Then the Zero doses have been measured (Background of pellet), and the average zero dose (ZD) has been calculated (with and without annealing) which in turn used to calculate Reader Calibration Factor (RCF) using the following equation:  $RCF = \frac{\text{Counts} - (\text{Average zero doses})}{\text{Dose of SSDL}}$  , where the conversion factor from (secondary standard dose laboratory) SSDL to dose equivalent were 1.21 and 1.2 for shallow dose Hp (0.07) and deep dose Hp (10) respectively.

Then the TLD chips irradiated by gamma radiation source (Cesium-137) and receiving 0 - 15 mGy, then the counts have been measured by TLDs with consideration to with/without annealing, used/unused nitrogen cooling and the usage of buildup i.e. calculation at shallow depth Hp (0.07) and deep depth Hp (10) and the obtained counts have been converted to dose at shallow and deep depths by applying the following formulas:  $H_p(0.07) = \text{counts } \mu\text{Gy} \times 1.21\text{mSv}$  and Deep dose  $H_p(10) = \text{counts } \mu\text{Gy} \times 1.21\text{mSv}$  Respectively.

### **3.3 Method of data analysis:**

The final data have been analyzed using Microsoft EXCELL.

## Chapter Four

### Results

The following section will highlight the results related to factors affecting the reading or the calibration of the TLD reader such as: reading of count/s with and without using filtration, with and without Nitrogen gas (cooling), with and without annealing (Zero dose reading) and the effect of dose in the chips structure. The results will be shown in forms of correlation, and bars.

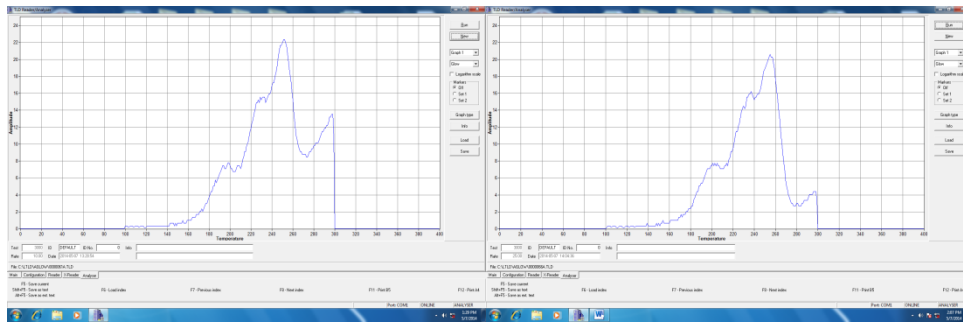


Figure 4.1: shows the glow curve spectrum in correlation between applied temperature in °C versus amplitude using filter Hp(0.07) at the right and Hp(10) at left side.

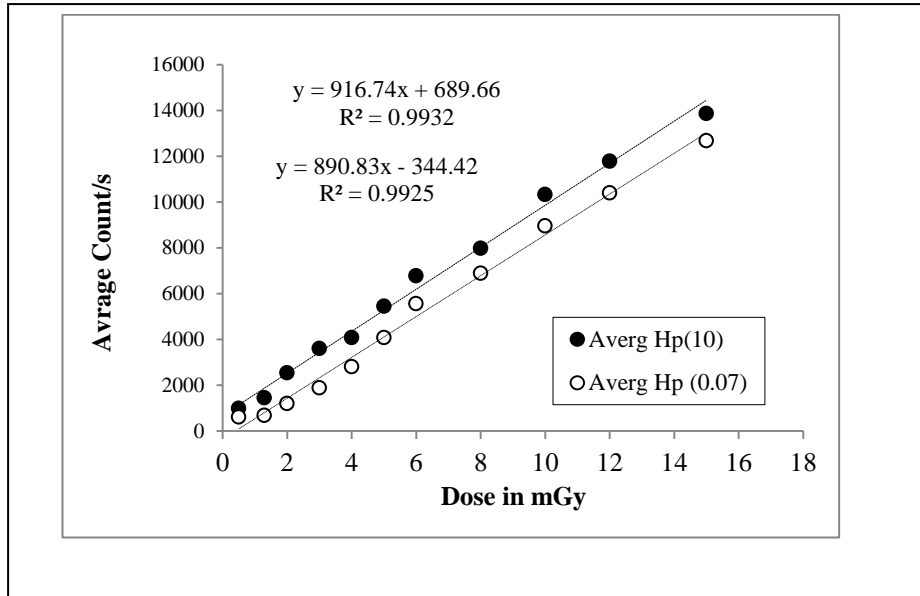


Figure 4.2: shows the correlation between applied dose in mGy and the relative TLD count/s using filter Hp(0.07) and Hp(10).

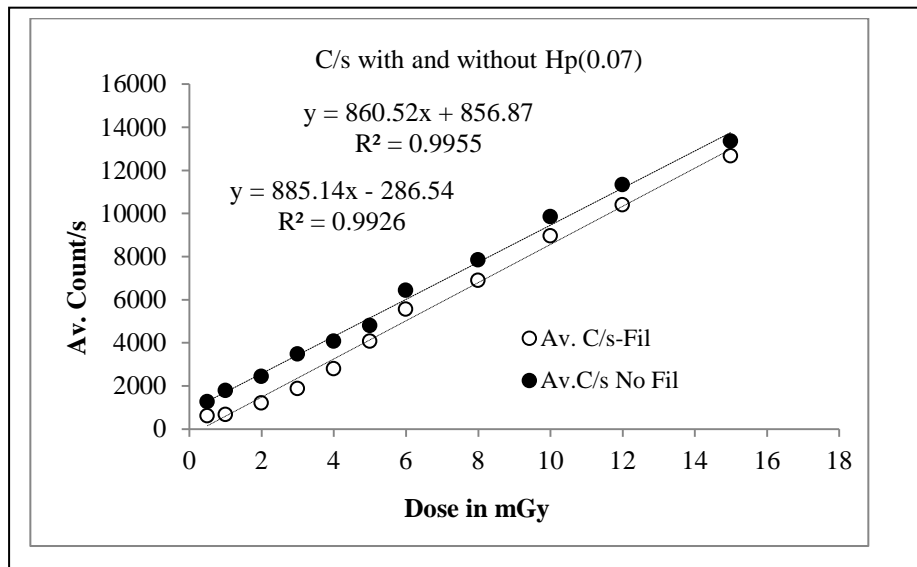


Figure 4.3: shows the correlation between the applied irradiation dose in mGy and the count/s of TLD chips with and without filter (Hp(0.07)).

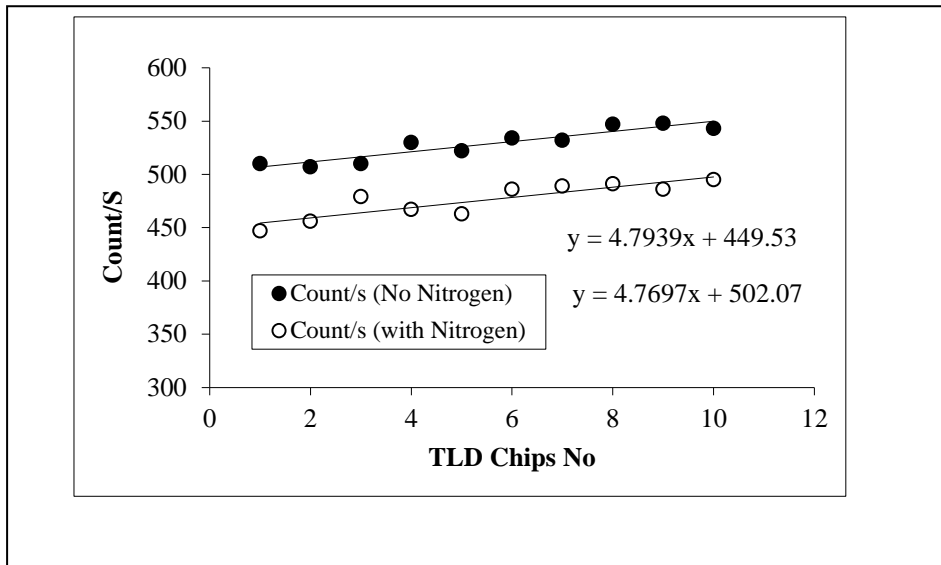


Figure 4.4: shows the correlation between the number of TLD chip and the count/s of TLD chips received equal dose (0.5 mGy) with and without Nitrogen flux for crystal cooling and no filter used.

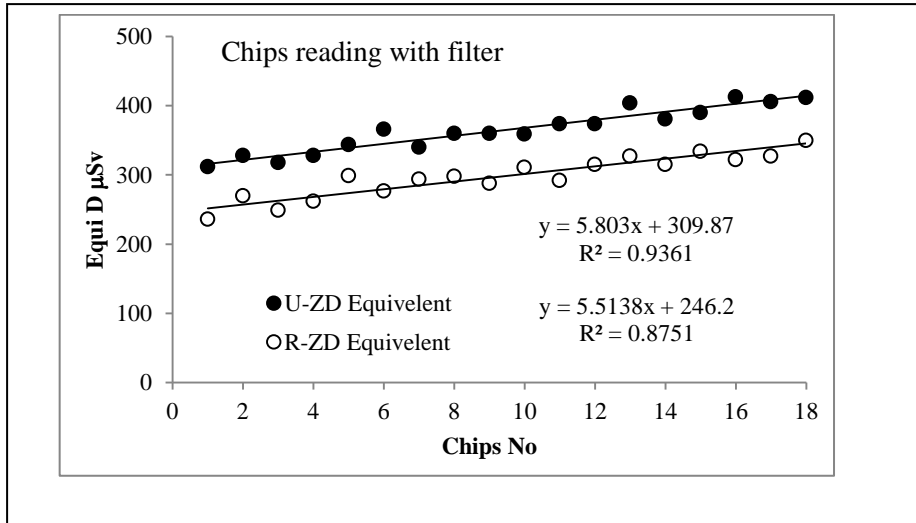


Figure 4.5: shows the correlation between the chips Number received equal dose and the dose in  $\mu\text{Sv}$  measured by TLD chips before and after annealing (with and without reading zero dose – with filter).

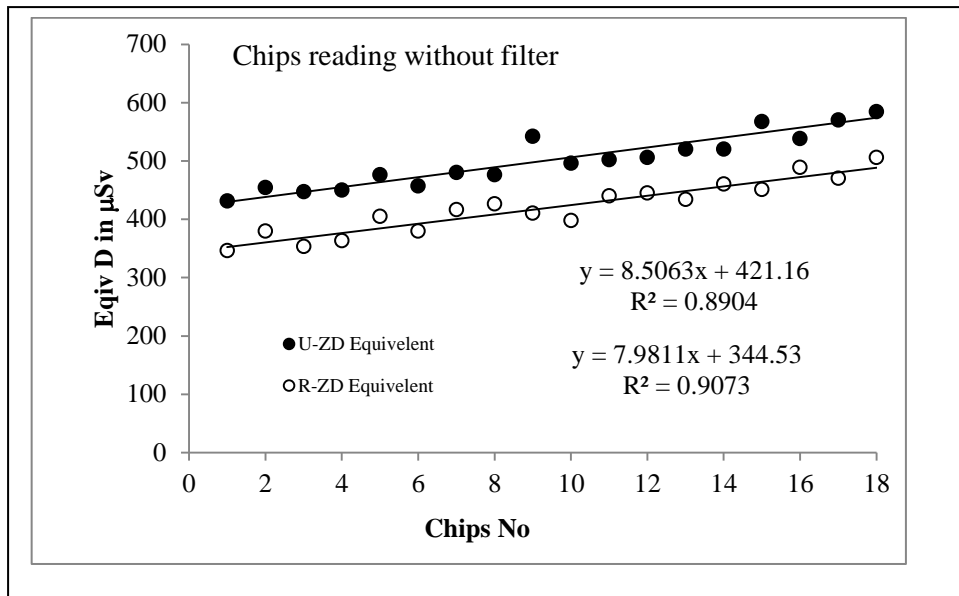


Figure 4.6: shows the correlation between the chips Number received equal dose and the dose in  $\mu\text{Sv}$  measured by TLD chips before and after annealing (without filter).

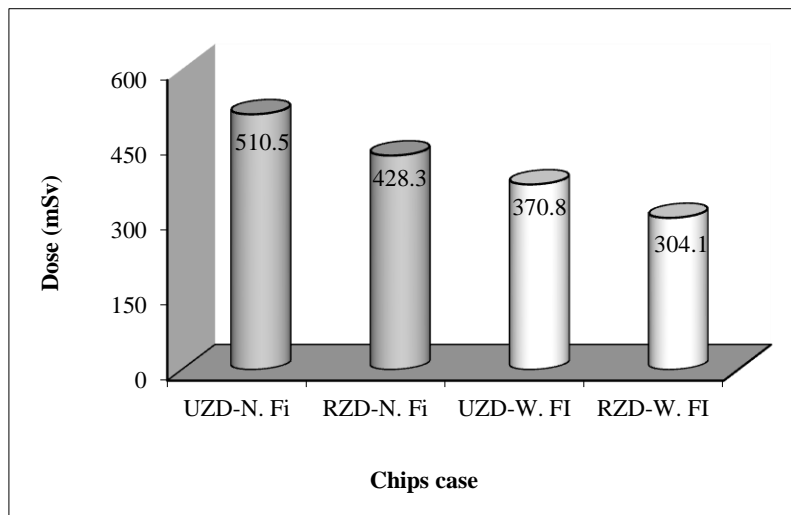


Figure 4.7: shows the dose in  $\mu\text{Sv}$  measured by TLD chips before and after annealing (with and without reading zero doses – with and without filter).



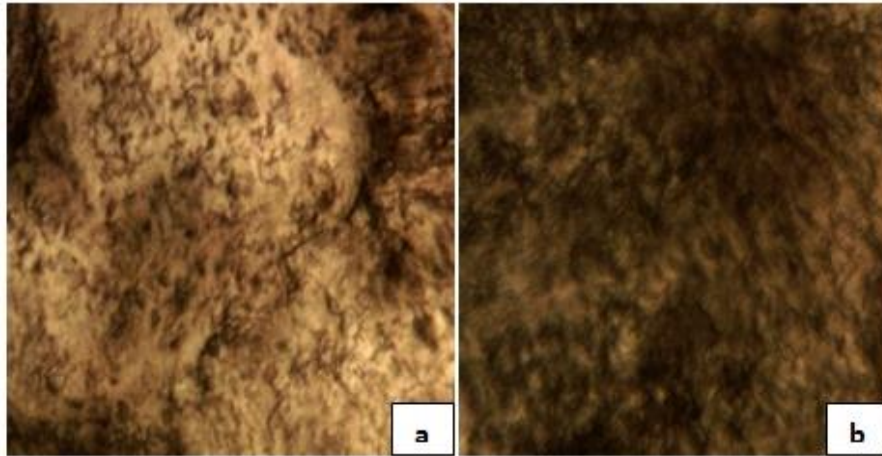


Figure 4.8: shows the scanning electron microscope image of LiF:Mg,Ti (a) annealed and before irradiation (b) annealed and after irradiation of 15 mGy.

## Chapter Five

### Discussion, Conclusion and Recommendation

#### 5.1 Discussion:

The following part is deal with the result discussion as appear in chapter four.

Figure (4.1) shows the glow curve spectrum in correlation between applied temperature in °C versus amplitude using (a) filter Hp (10) and (b) filter Hp (0.07).

Figure (4.2) shows correlation between the applied dose in mGy and the relative TLD count/s. The average TLD count/s with filter Hp (10) was greater than that obtained with filter Hp (0.07) with an amount of 1191 c/s, (19%) the high count at Hp (10) ascribed to the electronic range or the buildup region for  $\gamma$ -radiation whereas the count with Hp (0.07) refers to the count at the surface.

Also figure (4.3) shows the correlation between the applied irradiation dose in mGy and the count/s of TLD chips with and without filter Hp (0.07). The analysis reveals that: there was a proportional linear relationship between the applied dose and the TLD chips count for both cases with and without filter, and the correlation could be fitted in the form of equations:  $y = 885.1x - 286.5$  and  $y = 860.5x + 856.8$  for filtered and without filtered beam respectively, where x refers to applied dose in mGy and y refers to count/s.

Such increment in count ascribed to increasing applied radiation dose; however the average counts/s with filter and without filter were 5064.5 and 6059.1 respectively i.e. the count without filter was greater than that with filter by an amount of 994.5 C/s (16.4%). This result could be due to beam absorption.

Figure (4.4) shows the correlation between the number of TLD chip and the count/s of TLD chips received equal dose (0.5 mGy) with and without Nitrogen flux for crystal cooling and no filter used. The study also shows that: the average count/s without nitrogen flux was greater than with nitrogen count despite the dose received by TLD chips was equal (0.5 mGy) with an amount of 52.4 C/s (11%); such result indicates the importance of system cooling during operation. Also there was a notation that: the count/s increases slightly with the number of chips being read; such increment in reading of count could be ascribed to an optimum annealing of the previous exposure, as the annealing is a sensitive case process.

The figure (4.5) shows the correlation between the chips number received equal dose (0.5mGy) and the dose in  $\mu\text{Sv}$  measured by TLD chips before and after annealing (with and without reading zero dose-with filter).

It reveals that: the doses measured without annealing (unread of zero doses), was so greater than that measured after annealing (reading of zero doses); this is due to accumulation of dose in case of reading without annealing (without reading zero dose) as the annealing usually emptied and releasing the stored energy in the TLD chips . Such variation in dose measurement with and without annealing could be ascribed to special annealing technique (heating at 400°C for 1 h, quick cooling, then 80°C for 24 hours) required for LiF crystal and also due to spurious TL which influence the reading as well as the tribo-luminescence (Light  $\lambda = 500 - 600$  nm originate at TL crystal surface embedded near to gas at 300°C - 400°C); as in fact inert gas like N<sub>2</sub> allow the surface stored energy in the crystal release with light emission and as well the intrinsic thermoluminescence efficiency; as different crystals have different efficiency for instance: LiF, CaF<sub>2</sub>:Mn, and CaSO<sub>4</sub> have 0.039%, 0.44% and 1.2% respectively and the relative effective atomic number ( $Z_{\text{eff}}$ ) are: 8.31, 16.9, 15.62 respectively.

Figure (4.6) shows the correlation between the chips number received equal doses (0.5 mGy) and the dose in  $\mu\text{Sv}$  measured by TLD chips before and after annealing (with and without reading zero dose-Filtered).

It reveals that: the doses measured without annealing i.e. unread of zero doses, were so greater than that measured with annealing (reading of zero doses); this is due to accumulation of dose in case of reading without annealing (without reading zero dose) as the annealing usually emptied and releasing the stored energy in the TLD chips [20]. Also it was so obvious that: there was slightly increment in the dose as there were more chips being read, such increment could be ascribed to suboptimum annealing of the chips.

In figure (4.7) shows the dose in  $\mu\text{Sv}$  measured by TLD chips before and after annealing i.e. with and without zero dose reading (with and without filter). The data analysis reveals that: in case of TLD chips reading without annealing, usually gives greater dose ( $510.5 \mu\text{Gy}$ ) compared with chips reading with annealing ( $428.3 \mu\text{Gy}$ ) with notation that: there was no filter used; hence the annealing causes a reduction in dose by  $82.2 \mu\text{Gy}$ , although this amount of dose depends on the environment to which the TLD crystal exposed before being used in experiment, however in case of using filter before and after annealing, the chips reading were  $370.8$  and  $304.1 \mu\text{Gy}$  respectively i.e. there was  $66.7 \mu\text{Gy}$  as reduction due to filtration; therefore the analysis deduced that: the effect of annealing was greater than the effect of filtration.

Figure (4.8): shows the scanning electron microscope image of LiF:Mg:Ti (a) annealed and before irradiation (b) annealed and after irradiation of 15 Gy. It revealed that: the morphology of LiF:Mg:Ti crystal appeared as more clear with no darkening in its surface compared with that appeared in (b). In such view and since the high temperature would alter the thermoluminescence glow curve after irradiation, and as well the energy band gap ( $E_g$ ) for the TLD crystal influenced by irradiation i.e. the pure TLD crystal before irradiation, its  $E_g$  would be in the range of solid state, while after irradiation its  $E_g$  decreases to be in the range of semiconducting material due to immigration of electrons from valence band towards conduction band and trapped in the forbidden band; hence the assumption of radiation induce opacity and crystallization changes in TLD crystal are inevitable which are in turn will affect the accuracy of TLD crystal radiation measurement after long period of application or specific radiation dose.

## 5.2 Conclusion:

The radiation dosimetry is of paramount importance since the early days when they started to be used. The thermoluminescent dosimeters are one of the main types of dosimeter used because of its ease of handling, Possibility measures in places where others would not be possible, small dimensions and various types of material existents. This study revealed that factors such as temperature, pressure, long term radiation exposure and moisture have great effect in TLD reader.

According to the analyzed results of the following analyzes, the researcher could conclude that:

- TLD average count/second (C/s) with filter Hp (10) was greater than that obtained with filter Hp (0.07) with an amount of 1191 c/s (19%).
- The average C/s without filter Hp (0.07) was greater than that with filter by an amount of 994.5 C/s (16.4%).
- There was proportional linear relationship; as the applied dose increased the TLD C/s increased significantly ( $R^2 = 0.9$ ) based on the equations:  $y = 885.1x - 286.5$  and  $y = 860.5x + 856.8$  for filtered and without filtered beam respectively, where x refers to applied dose in mGy and y refers to C/s.
- Also the average C/s without nitrogen flux (cooling) was greater than with nitrogen count with an amount of 52.4 C/s (11%). The

annealing (without filter) causes a reduction in dose by 82.2  $\mu\text{Gy}$  (19.2%), and in case of annealing with filter, the dose reduced by 66.7  $\mu\text{Gy}$  (21.9%) relative to annealing without filter.

- Themorphology of TLD crystal was a darkening surface after irradiation



### **5.3 Recommendations:**

- We recommended for quality assurance of recalibration has to be considered for accuracy and sensitivity of TLD.
- We recommended repeating annealing in several times to remove the impurities.
- The availability is very important as well as the stability of its produced signal.
- We recommended using modern techniques to study factors affect TLD reader.

## References:

Al-Haj, A.N. and Lagarde, C.S. (2004) Glow Curve Evaluation in Routine Personal Dosimetry. *Health Physics* 86, S15-S19. <https://doi.org/10.1097/00004032-200402001-00007>.

Asri, M. M. Teridi. 2005. Radiation and temperature effects on conductivity and dielectric properties of poly (vinyl alcohol)-potassium hydroxide-propylene carbonate. Dissertation, Master Thesis. Physics Department, University Putra Malaysia.

Attix, F, H, Introduction to Radiological Physics & Radiation Dosimetry, Canada: John Wiley & Sons, 1986.

Attix, F. (2004) Introduction to Radiological Physics and Radiation Dosimetry. Wiley, Hoboken.

Barlow W (1883). "Probable nature of the internal symmetry of crystals". *Nature* 29 (738): 186. Bibcode:1883Natur..29..186B. doi:10.1038/029186a0. See also

Barlow, William (1883). "Probable Nature of the Internal Symmetry of Crystals". *Nature* 29 (739): 205. Bibcode:1883Natur..29..205B. doi:10.1038/029205a0.

Sohncke, L. (1884). "Probable Nature of the Internal Symmetry of Crystals". *Nature* 29 (747): 383. Bibcode:1884Natur..29..383S. doi:10.1038/029383a0.

Barlow, WM. (1884). "Probable Nature of the Internal Symmetry of Crystals". *Nature* 29 (748): 404. Bibcode:1884Natur..29..404B. doi:10.1038/029404b0.

Bhat, N.V., M.M. Nate, M.B. Kurup, V.A. Bambole, S. Sabharwal. 2005. Effect of  $\gamma$ -radiation on the structure and morphology of polyvinyl alcohol films. *Nuclear Instruments and Methods in Physics Research B* 237: 585-592.

Bilskia, P., Bergerb, T., Hajekc, M., Twardaka, A., Koernerb, C. and Reitz, G. (2013) Thermoluminescence Fading Studies: Implications for Long-Duration Space Measurements in Low Earth Orbit. *Radiation Measurements* , 56, 303-306.<https://doi.org/10.1016/j.radmeas.2013.01.045>.

Bos, A.J. (2001) High Sensitivity Thermoluminescent Dosimetry. *Nuclear Instruments and Methods in Physics Research Section B* , 184, 3-28.[https://doi.org/10.1016/S0168-583X\(01\)00717-0](https://doi.org/10.1016/S0168-583X(01)00717-0).

Bragg (1913). "The Structure of Some Crystals as Indicated by their Diffraction of X-rays". *Proc. R. Soc. Lond. A* 89 (610): 248–277. JSTOR93488.

Bragg (1914). "Die Reflexion der Röntgenstrahlen". *Jahrbuch der Radioaktivität und Elektronik* 11: 350.

Bragg WH (1907). "The nature of Röntgen rays". *Transactions of the Royal Society of Science of Australia* 31: 94.

Bragg WH (1908). "The nature of  $\gamma$ - and X-rays". *Nature* 77 (1995): 270. Bibcode:1908Natur..77..270B. doi:10.1038/077270a0. See also Bragg, W. H. (1908). "The Nature of the  $\gamma$  and X-Rays". *Nature* 78 (2021): 271. Bibcode:1908Natur..78..271B. doi:10.1038/078271a0. Bragg, W. H. (1908). "The Nature of the  $\gamma$  and X-Rays". *Nature* 78 (2022): 293. Bibcode:1908Natur..78..293B. doi:10.1038/078293d0. Bragg, W. H. (1908). "The

Nature of X-Rays". Nature 78 (2035): 665.

Bibcode:1908Natur..78R.665B.doi:10.1038/078665b0.

Bragg WH (1910). "The consequences of the corpuscular hypothesis of the  $\gamma$ - and X-rays, and the range of  $\beta$ -rays". Phil. Mag. 20 (117): 385. doi:10.1080/14786441008636917.

Bragg WH (1912). "On the direct or indirect nature of the ionization by X-rays". Phil. Mag. 23 (136): 647. doi:10.1080/14786440408637253.

Bragg WH, Bragg WL (1913). "The structure of the diamond". Nature 91 (2283): 557. Bibcode:1913Natur..91..557B. doi:10.1038/091557a0.

Bragg WH, Bragg WL (1913). "The structure of the diamond". Proc. R. Soc. Lond. A89 (610): 277. Bibcode:1913RSPSA..89..277B. doi:10.1098/rspa.1913.0084.

Bragg WL (1912). "The Specular Reflexion of X-rays". Nature 90 (2250): 410. Bibcode:1912Natur..90..410B. doi:10.1038/090410b0.

Bragg WL (1913). "The Diffraction of Short Electromagnetic Waves by a Crystal". Proceedings of the Cambridge Philosophical Society 17: 43.

Bragg WL (1914). "The analysis of crystals by the X-ray spectrometer". Proc. R. Soc. Lond. A89 (613): 468. Bibcode:1914RSPSA..89..468B. doi:10.1098/rspa.1914.0015.

Bragg WL (1914). "The Crystalline Structure of Copper". *Phil. Mag.* 28 (165): 355. doi:10.1080/14786440908635219.

Bragg WL, James RW, Bosanquet CH (1921). "The Intensity of Reflexion of X-rays by Rock-Salt". *Phil. Mag.* 41 (243): 309. doi:10.1080/14786442108636225.

Bragg WL, James RW, Bosanquet CH (1921). "The Intensity of Reflexion of X-rays by Rock-Salt. Part II". *Phil. Mag.* 42 (247): 1. doi:10.1080/14786442108633730.

Bragg WL, James RW, Bosanquet CH (1922). "The Distribution of Electrons around the Nucleus in the Sodium and Chlorine Atoms". *Phil. Mag.* 44 (261): 433. doi:10.1080/14786440908565188.

Bravais A (1850). "Mémoires sur les systèmes formés par des points distribués régulièrement sur un plan ou dans l'espace". *Journal de l'Ecole Polytechnique* 19: 1.

Compton A (1923). "A Quantum Theory of the Scattering of X-rays by Light Elements". *Phys. Rev.* 21 (5): 483. Bibcode:1923PhRv...21..483C. doi:10.1103/PhysRev.21.483.

Dahoud, M. and Mustafa, I. (2014) Radiation Dosimetry by TLDs Inside Human Body Phantom While Using <sup>192</sup>Ir HDR in Breast Brachytherapy. *International Journal of Scientific & Technology Research* , 3, 172-176.

Dam, J, V, and Morenello, G, Methods for in vivo dosimetry in external radiotherapy, 2nd ed. Brussels: ESTRO, 2006.

Dana ES, Ford WE (1932). A Textbook of Mineralogy, fourth edition. New York: John Wiley & Sons. p. 28.

Dey, K., Ganguli, S., Ghoshal, S., Khan, M.A. and Khan, R.A. (2014) Study of the Effect of Gamma Irradiation on the Mechanical Properties of Polyvinyl Alcohol Based Gelatin Blend Film. Open Access Library Journal, 1: e639. DOI: 10.4236/oalib.1100639

Einstein A (1905). "Übereinen die Erzeugung und Verwandlung des LichtesbetreffendenheuristischenGesichtspunkt (trans. A Heuristic Model of the Creation and Transformation of Light)".Annalen der Physik 17 (6): 132. Bibcode:1905AnP...322..132E. doi:10.1002/andp.19053220607. (German). An English translation is available from Wikisource.

Einstein A (1909). "Über die EntwicklungunsererAnschauungenüber das Wesen und die Konstitution der Strahlung (trans. The Development of Our Views on the Composition and Essence of Radiation)".PhysikalischeZeitschrift 10: 817. (German). An English translation is available from Wikisource.

ENVIRONMENT AGENCY UK Radioactivity in Food and the Environment, 2012.

Evan, R.D. 1952. The Atomic Nucleus McGraw-Hill, New York.

Faiz M. Khan (2003). "The Physics of Radiation Therapy".Lippincott Williams & Wilkins.

Faiz, K. (2010), The Physics of Radiation Therapy. 4th Edition, Lippincott Williams & Wilkins, Philadelphia.

Fowler J. F. and F. H. Attix.(1966). Solid state integrating dosimeters. Radiation dosimetry (Edited by F. H. ATTIX and W. C. ROESCH) 2<sup>nd</sup>. Edition, Vol. 2, Chap. 14 Academic Press.

Fowler J. F. and F. H. Attix.(1966). Solid state integrating dosimeters. Radiation dosimetry (Edited by F. H. ATTIX and W. C. ROESCH) 2<sup>nd</sup>. Edition, Vol. 2, Chap. 14 Academic Press.

Fowler, J.F. and Attix, F.H. (1966) Solid State Integrating Dosimeters. In: Attix, F.H. and Roesch, W.C., Eds., Radiation Dosimetry , 2nd Edition, Vol. 2, Academic Press, New York, Chap. 14.

Fried Joel R. (2014). Polymer Science and Technology, 3rd. edition. Prentice Hall, Professional Technical Reference: Upper Saddle River, NJ, 2003. 582 pp. ISBN 0130181684.

Friedrich W, Knipping P, von Laue M (1912). "Interferenz-Erscheinungen bei Röntgenstrahlen". Sitzungsberichte der Mathematisch-Physikalischen Classe der Königlich-Bayerischen Akademie der Wissenschaften zu München 1912: 303.

Hessel JFC (1831). Kristallometrie oder Kristallonomie und Kristallographie. Leipzig.

Hossam M. Said. (2013). Effects of gamma irradiation on the crystallization, thermal and mechanical properties of poly(L-lactic acid)/ethylene-covinyl acetate blends, *Journal of radiation research and applied sciences*, vol. 6, P: 11-20.

[https://www.ndeed.org/EducationResources/CommunityCollege/RadiationSafety/radiation\\_safety\\_equipment/thermoluminescent.htm](https://www.ndeed.org/EducationResources/CommunityCollege/RadiationSafety/radiation_safety_equipment/thermoluminescent.htm)

I. A. Bochvar, T. I. Gimadova, I. B. Keirim-Markus, et al., *Method of X-Ray Dosimetry* [in Russian], Atomizdat, Moscow (1977).

IAEA, *Practical Radiation Technical Manual – Individual monitoring*, Vienna: IAEA, 2004.

IAEA, *Radiation Oncology Physics: A handbook for teachers and students*, Vienna: IAEA, 2005.

ICRP report 103 para 104 and 105.

Kalidasan, M., Asokan, K., Baskar, K., Dhanasekaran, R. (2015). Effect of gamma ray irradiation on sodium borate single crystals. *Radiation Physics and Chemistry*, Vol. 117, P: 70-77. DOI: 10.1016/j.radphyschem.2015.07.016

Kepler J (1611). *Strenaseu de NiveSexangula*. Frankfurt: G. Tampach. ISBN3-321-00021-0.

Kitis, G. and Tuyn, J.W.N.A. (1998) Simple Method to Correct for the Temperature Lag in TL Glow-Curve Measurements. *Journal of Physics, D: Applied Physics*, 31, 2065-2073. <https://doi.org/10.1088/0022-3727/31/16/017>.

Knoll, G, F, *Radiation Detection & Measurement*, 3rd ed, United States of America: John Wiley & Sons, 2000.



Laue M (1914). "Concerning the detection of x-ray interferences" (PDF). Nobel Lectures, Physics. 1901–1921. Retrieved 2009-02-18.

Lee, Y., Won, Y. and Kang, K. (2015) A Method to Minimize the Fading Effects of LiF:Mg,Ti (TLD-600 and TLD-700) Using a Pre-Heat Technique. Radiation Protection Dosimetry, 164, 449-455. <https://doi.org/10.1093/rpd/ncu302>.

Leon, B.W. (2009) Using Thermoluminescent Dosimeters to Measure the Dose from High and Low Energy X-Ray Sources. UNLV Theses, Dissertations, Professional Papers, and Capstones, Paper 1203.

Lucke, W.C. (1970) Intrinsic Efficiency of Thermoluminescent Dosimetry Phosphors. Report 7104, Naval Research Laboratory, Washington DC.

McKinlay, A, F, Thermoluminescence dosimetry-Medical Physics Handbooks 5, Bristol: Adam Hilger Ltd, 1981.

Mohammed A. Ali Omer, Abdulrahman A. Alsayyari, Jumaa Y. Tamboul, Rowida B. Ali, Amira A. Ahmed, Ahmed Abukonna. (2017). Studying of Common Factors Affecting Reading of Lithium Fluoride Thermoluminescence Dosimeter Crystal. Open Journal of Biophysics, 7, P:14-24. DOI: 10.4236/ojbiphy.2017.71002

Mohammed Amed Ali Omer, Elias Saion, Khairul Zaman Dahlan. (2011). Radiation Synthesis of Conducting Polyaniline and PANI/Ag Nanocomposites: Radiation Synthesis of Conducting Polymer, Lambert-Academic Publisher-German, ISBN: 3845418672, 9783845418674.

Pais A (1982). *Subtle is the Lord: The Science and the Life of Albert Einstein*. Oxford University Press. ISBN0-19-853907-X.

Pradhan A.S., Gopalakrishnan, A.K. and Iyer, P.S. (1992) Dose Measurement at High Atomic Number Interfaces in Megavoltage Photon Beams Using TLDs. *Medical Physics* ,19, 355-356. <https://doi.org/10.1118/1.596909>.

Pradhan, A.S. and Bhatt, R.C. (1979) Metal Filters for the Compensation of Photon Energy Dependence of the Response of CaSO<sub>4</sub>: Dy-Teflon TLD Discs. *Nuclear Instrumentation and Methods*,166,497-501.[https://doi.org/10.1016/0029-554X\(79\)90540-8](https://doi.org/10.1016/0029-554X(79)90540-8).

Sandra R. Scagliusi, Elisabeth C. L. Cardoso, Cristina A. Pozenato and Ademar B. Lugaõ. (2013). Degrading radiation effects on properties of bromobutyl rubber compounds. *International Nuclear Atlantic Conference – INAC*, P: 24-29.

Savva, A. (2010) *Personnel TLD Monitors, Their Calibration and Response*. MSc Dissertation, University of Surrey, Guildford.

Schönflies A (1891). *Kristallsysteme und Kristallstruktur*. Leipzig.

Sen, C. Uzun, K. Glu, S.M.E. Gan, V. Deniz, O. G. Evren.(2003). Effect of gamma irradiation conditions on the radiation-induced degradation of isobutylene–isoprene rubber. *Nuclear Instruments and Methods in Physics Research B* 208, 480–484.

Shafranovskii I I and Belov N V (1962). "E. S. Fedorov". *50 Years of X-Ray Diffraction*, ed. Paul Ewald (Springer): 351. ISBN90-277-9029-9.

Stadtman, H., Delgado, A. and Go'mez-Ros, J.M. (2002) Study of Real Heating Profiles in Routine TLD Readout: Influences of Temperature Lags and Non-Linearities in the Heating Profiles on the Glow Curve Shape. *Radiation Protection Dosimetry* , 101, 141–144.<https://doi.org/10.1097/00004032-200402001-00007>.

Stadtman, H., Hranitzky, C. and Brasik, N. (2006) Study of Real Time Temperature Profiles in Routine TLD Read Out—Influences of Detector Thickness and Heating Rate on Glow Curve Shape. *Radiation Protection Dosimetry*, 119, 310-313. <https://doi.org/10.1093/rpd/nci655>. StenoN (1669). *De solido intra solidum naturaliter contento dissertationis prodromus*. Florentiae.

The ICRP says "In the low dose range, below about 100 mSv, it is scientifically plausible to assume that the incidence of cancer or heritable effects will rise in direct proportion to an increase in the equivalent dose in the relevant organs and tissues" ICRP publication 103 paragraph 64

Tochilin, E., Goldstein, N. and Miller, W.G. (1969) Beryllium Oxide as a Thermoluminescent Dosimeter. *Health Physics* , 16, 1-7.<https://doi.org/10.1097/00004032-196901000-00001>.

Tochilin, E., N. Goldstein, and W. G. Miller."Beryllium oxide as a thermoluminescent dosimeter." *Health physics* 16.1 (1969): 1-7.

Tochilin, E., N. Goldstein, and W. G. Miller."Beryllium oxide as a thermoluminescent dosimeter." *Health physics* 16.1 (1969): 1-7.

Toktamiş, H. and NecmeddinYazici, A. (2012) Effects of Annealing on Thermoluminescence Peak Positions and Trap Depths of Synthetic and Natural

Quartz by Means of the Various Heating Rate Method. Chinese Physics Letters , 29, Article ID: 087802.<https://doi.org/10.1088/0256-307X/29/8/087802>.

United Nations Scientific Committee on the Effects of Atomic Radiation Annex E: Medical radiation exposures – Sources and Effects of Ionizing – 1993, p. 249, New York, UN.

Yamashita, T., N. Nada, H. Onishi and S. Kitamura."Calcium sulfate activated by thulium or dysprosium for thermo-luminescence dosimetry." Health physics vol. 21(2), (1971): 295-300.

Yamashita, T., N. Nada, H. Onishi and S. Kitamura."Calcium sulfate activated by thulium or dysprosium for thermo-luminescence dosimetry." Health physics vol. 21(2), (1971): 295-300.

Yamashita, T., Nada, N., Onishi, H. and Kitamura, S. (1971) Calcium Sulfate Activated by Thulium or Dysprosium for Thermoluminescence Dosimetry. Health Physics , 21, 295-300.<https://doi.org/10.1097/00004032-197108000-00016>.

Zimmerman, D.W., Rhyner, C.R. and Cameron, J. (1966) Thermal Annealing Effects on the Thermoluminescence of LiF. Health Physics , 12, 525-531.<https://doi.org/10.1097/00004032-196604000-00007>.

## Appendix A:

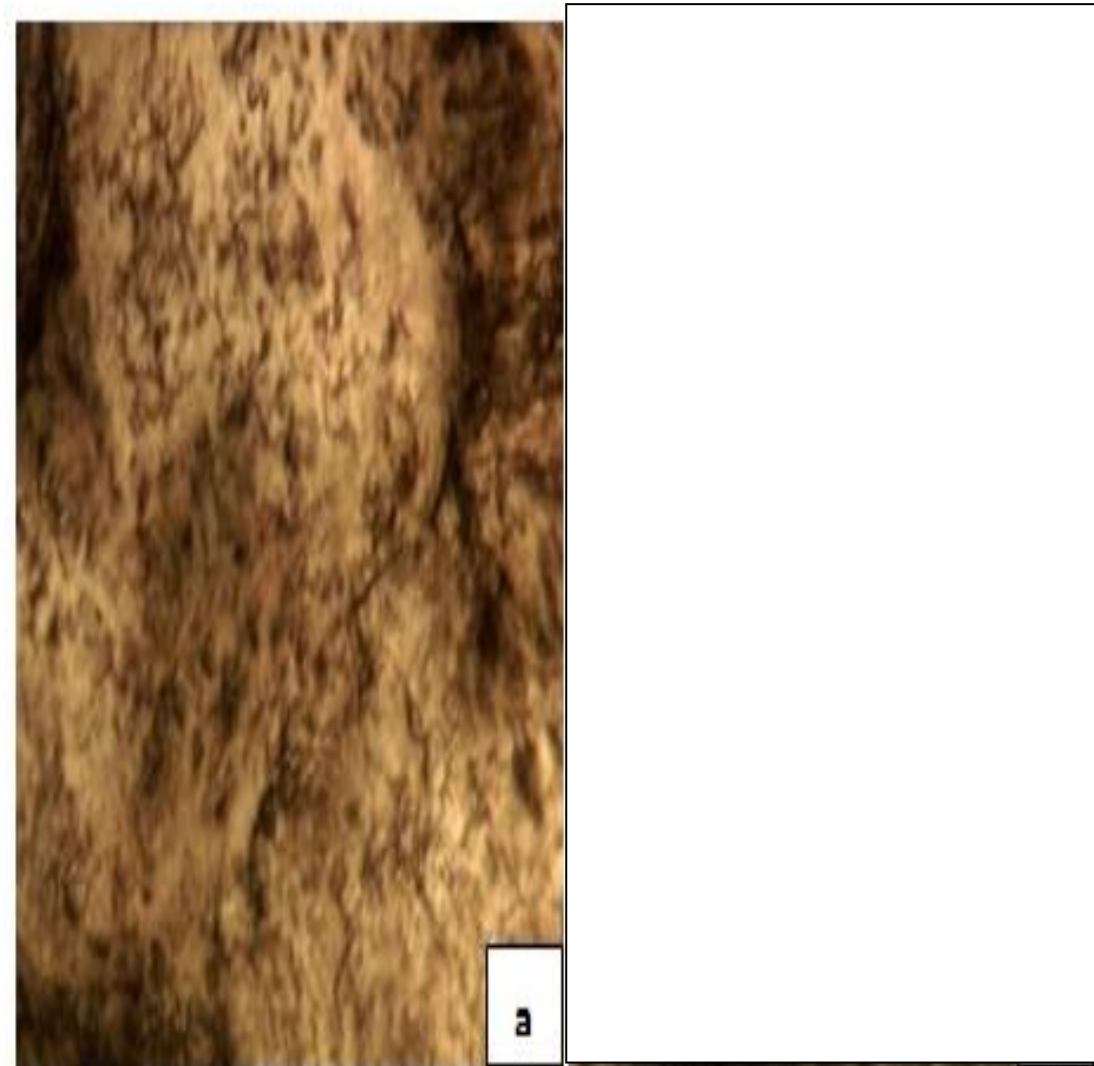


**Figure 1:** shows the scanning electron microscope image of LiF:Mg,Ti (a) annealed and before irradiation .



**Figure 1:** shows the scanning electron microscope image of LiF:Mg,Ti annealed and after irradiation of 15 mGy.

# **Published Scientifics paper**